RIGOROUS SIMULATION OF ACCIDENTAL LEAKS FROM HIGH-PRESSURE STORAGE VESSELS

A Thesis

by

ALISHA

Submitted to the Office of Graduate and Professional Studies of
Texas A&M University
in partial fulfillment of the requirements for the degree of

MASTER OF SCIENCE

Chair of Committee,	Marcelo Castier
Co-Chair of Committee,	Luc Nicholas Véchot
Committee Members,	Vassilios Kelessidis
Head of Department,	M. Nazmul Karim

August 2014

Major Subject: Chemical Engineering

ABSTRACT

Several major industrial disasters involve accidental releases of hazardous chemicals from ruptured vessels or pipelines as consequence of equipment failures, maintenance errors, operational errors, cracks, corrosion, ruptures, or also by acts of nature. The released chemical can form and disperse as vapor cloud leading to fire, explosion, or toxic exposure. The resulting leak could be single phase or multiphase release, choked or non-choked. These releases could result in liquid spills, vapor cloud formation, explosion, toxic dispersion and flashing liquids. The impact of the release depends on the properties of the fluid and the exit conditions. Often the leak goes unnoticed and also it becomes hard to estimate the leak flow rate. When a leak occurs, it is very important to have an idea of the leak flow rate and the fluid properties. This helps in assessing the hazards posed by the leak and also predict the consequences.

To assess the consequences of a leak, it is important to estimate its flow rate and properties of the discharged fluid, but both change with time during the leaking process. Several models and programs exist to simulate accidental releases, often based on assumptions that increase the uncertainty of their predictions when applied to high-pressure vessels. This thesis takes a different approach by using rigorous calculation procedures and a cubic equation of state to: (1) find the state of fluid within the vessel using a flash algorithm for systems of specified internal energy (U), volume (V), and mole numbers of each component (N); (2) track phase appearance and disappearance in the vessel; (3) find the state of fluid as it exits the vessel, assuming the leaking point is

the throat of an adiabatic, converging nozzle that operates isentropically; (4) compute sound speeds in multiphase systems to establish whether the leak flow is choked. The code that implements these steps has been validated against ideal gas state for single component data and against experimental data for leaks from vessels containing mixtures.

ACKNOWLEDGEMENTS

I would like to thank my committee chair, Dr. Marcelo Castier, and my committee members, Dr. Luc N Véchot and Dr. Vassilios Kelessidis, for their guidance and support throughout the course of this research.

Thanks also go to my friends and colleagues and the department faculty and staff for making my time at Texas A&M University at Qatar a great experience. I also want to extend my gratitude to the Itochu Corporation, who supported my M.S.

Finally, thanks to my parents for their encouragement and to my husband for his patience, love and unconditional support.

NOMENCLATURE

A_c	Cross sectional area along the length of the vessel (m^2)
A_h	Cross sectional area at height 'h' (m^2)
A_{hole}	Area of the hole (m^2)
A_s	Area of nozzle's exit plane (m^2)
A_t	Area of the tank (m^2)
b	Breadth of the rectangular hole (m)
c_s	Speed of sound (m/s)
C_o	Coefficient of discharge
C_v	Heat capacity at constant volume ($J/K.m^3$)
d	Diameter of the vessel/hole (m)
g	Acceleration due to gravity (m/s^2)
G_c	Critical mass flux ($kg/m^2.s$)
G_{CL}	Critical mass flux with low inlet quality ($kg/m^2.s$)
G_L	Mass flux of all-liquid flow ($kg/m^2.s$)
G_{ERM}	Equilibrium rate model flux ($kg/m^2.s$)
h	Height of fluid in the vessel (m)
h_0	Initial height of fluid in the vessel (m)
h_{fluid}	Enthalpy per unit mass of the fluid (J/kg)
$h_{j,in\text{-}tank}$	Molar enthalpy of stream 'j' entering the vessel (J/mol)
$h_{k,out\text{-}tank}$	Molar enthalpy of stream 'k' exiting the vessel (J/mol)

$h_{in-nozzle}$	Molar enthalpy of stream entering the nozzle (J/mol)
$h_{out-nozzle}$	Molar enthalpy of stream exiting the nozzle (J/mol)
h_{rh}	Upper limit of rupture (m)
h_{rl}	Lower limit of rupture (m)
h_s	Molar enthalpy of fluid entering the nozzle from the tank (J/mol)
h_t	Molar enthalpy of fluid at the nozzle's exit plane(J/mol)
h_{ex}	Enthalpy per unit mass of the fluid at the exit throat (J/kg)
L	Length of the vessel (m)
M	Molecular weight of the escaping vapor or gas (g/mol)
$M_{out-nozzle}$	Mass of stream exiting the nozzle (g)
M_s	Molar mass of leaking fluid at nozzle's exit plane (g/mol)
$n_{i,in}$	Number of moles of component i in the inlet (mol)
$n_{i,out}$	Number of moles of component i in the outlet (mol)
$\dot{n}_s$	Molar flow rate (mol/s)
N_i	Total number of moles of component i (mol)
N_o	Initial number of moles (mol)
P	Pressure at the throat (Pa)
P_{atm}	Atmospheric pressure (Pa)
P_o	Pressure within the vessel (Pa)
$P_{out-nozzle}$	Pressure of stream exiting the nozzle (Pa)
P_s	Pressure of leaking fluid at nozzle's exit plane (Pa)
$\dot{Q}$	Heat transfer rate to the vessel (J/s)

r	Radius of the vessel (m)
r_c	Radius of the circular hole (m)
rh	Rupture high (m)
rl	Rupture low (m)
R	Ideal gas constant (Pa.m^3/mol.K)
$s_{in-nozzle}$	Molar entropy of stream entering the nozzle (J/mol.K)
$s_{out-nozzle}$	Molar entropy of stream exiting the nozzle (J/mol.K)
s_s	Molar entropy of leaking fluid at nozzle's exit plane (J/mol.K)
s_t	Molar entropy of fluid entering the nozzle from tank (J/mol.K)
t	Time (s)
t_e	Emptying time of the vessel till it reaches the leak height (s)
t_f	Final time (s)
T	Temperature of the fluid in the vessel (K)
T_o	Initial temperature of the fluid in the vessel (K)
$T_{out-nozzle}$	Temperature of stream exiting the nozzle (K)
T_s	Temperature of the source (K)
$u_{out-nozzle}$	Velocity of stream exiting the nozzle (m/s)
u_s	Velocity of leaking fluid (m/s)
U	Total Internal energy (J)
v_{ex}	Velocity of the fluid at the exit throat (m/s)
v_g	Specific volume of the gas
v_s	Molar volume of mixture at nozzle's exit plane (m^3/mol)

V	Volume (m^3)
V_1	Volume of phase 1 (m^3)
V_2	Volume of phase 2 (m^3)
V_{rh}	Volume of the fluid at rh (m^3)
V_{rl}	Volume of the fluid at rl (m^3)
W	Shaft work (J)
x	Quality

Other symbols

γ	Heat capacity ratio
ρ	Density (kg/m^3)
η	Critical pressure ratio
ϕ	Vessel diameter (m)

TABLE OF CONTENTS

Page

LIST OF FIGURES

Page

LIST OF TABLES

1. INTRODUCTION

In the process industry, major disasters have been caused by the accidental (uncontrolled) release of hazardous chemicals. The formation and dispersion of vapor clouds following these releases can result in fire, explosion and toxic exposure. The release of hazardous chemical can be caused by leaks in process equipment following equipment failures, maintenance errors, operational errors, cracks, corrosion, ruptures, or also by acts of nature.

To assess the consequences of a leak it is very important to estimate its flow rate and the properties of the fluid as it exits the ruptured pipeline or vessel. The release can be single phase or multiphase release, choked or non-choked. Thus, the calculation of the release rate involves the assessment of the speed, composition and number of phases of the fluid as it leaves the vessel. It is equally important to assess how the properties of the fluid remaining inside the vessel change as function of time during the leaking period. The properties of interest include the temperature, pressure, amount of each chemical component, and number of phases inside the vessel, as well as their state of aggregation (solid, liquid, or vapor). The properties of the leaking fluid and the fluid in the vessel are key to understand the dynamic behavior of the vessel depressurization process. Given the practical importance of this subject and the theoretical challenges of its mathematical modeling, there has been much work in this area, including models and computational programs to simulate leaks from vessels and pipelines. Some of them embed assumptions about physical property behavior, such as the ideal gas equation of

state, that increase the uncertainty of their predictions when applied to high pressure leaking vessels.

This thesis work focuses on the simulation of leaks resulting from cracks or ruptures in high pressure storage vessels. A code is developed in the Fortran language that carries out several thermodynamic calculations to compute the flow rate of the leak. The code developed takes into account the phenomena of choked or non-choked flows. The program carries out flash calculations at specified values of internal energy (U), volume (V), and mole numbers of each component (N) (UVN flash) to determine the state of the fluid inside the tank. The leaking point is assumed to be the throat of an adiabatic, converging nozzle that operates isentropically. The mass and energy balances in the nozzle, along with isentropic flow condition and sound speed calculations, allow the identification of the flow as choked or not and the computation of its flow rate and thermodynamic properties. The program accounts for different tank and hole geometries and also phase appearance and disappearance. It has been validated against ideal gas state for single component single phase system and against experimental data for leaks of multicomponent systems.

The next section 'Literature review', discusses literature work on simulation of accidental fluid releases. This is followed by section 3 that gives an overview of the scope of work. Section 4 then describes the methodology involved in developing the procedure for dynamic simulation of fluid releases. Section 5 discusses the tests and examples carried out for validation of the procedure, which is followed by Conclusion.

2. LITERATURE REVIEW

The literature on accidental fluid releases and their simulation is vast. This section reviews part of it, focusing on vessel depressurization, the factors that affect it, its consequences, and existing computer programs to simulate it. The final section comments on the source of the algorithms used in the simulator developed in this thesis.

2.1 Depressurization

When there is a sudden rupture in a pressurized tank, the fluid within leaks out to the atmosphere, which is followed by a pressure drop within the tank. This pressure change is called as depressurization. At first, there is a sharp initial decay in pressure due to release of the fluid within the vessel. The pressure gradient at the point of leak accelerates the fluid through the rupture (Lenclud & Venart, 1996).

In the process of depressurization, when the fluid leaks out of the high pressure vessel, if the process is adiabatic, this may result in very low temperatures of the fluid leaking out to the atmosphere (Haque, Richardson, Saville, & Chamberlain, 1990).

When a leak starts, the fluid's initial acceleration may take it to a condition in which the fluid velocity equals the sound speed of the exiting fluid. The fluid flow is said to be in choking conditions, under which, the fluid velocity is independent of the downstream conditions. Hence, it is important to predict when the flow reaches choking conditions. If the fluid is liquid, upon reaching the saturation boundary, it may flash and the fluid becomes a two-phase mixture. Gradually, the difference between the internal pressure and pressure at the exit of the fluid decreases and the flow becomes subsonic.

The fluid flow gradually changes from turbulent to laminar until there is no flow and the pressure inside and outside the vessel become equal (Lenclud & Venart, 1996).

When the fluid is released from the vessel, the fluid temperature within the vessel decreases due to decrease in the vessel pressure. However, there is heat transfer from the vessel wall to the fluid. These two simultaneous effects complicate the fluid behavior during depressurization (Xia, Smith, & Yadigaroglu, 1993).

2.2 Factors affecting depressurization

The factors affecting the behavior of the fluid in the event of an accidental release are (Cumber, 2001):

- Initial pressure within the tank
- Temperature of the fluid
- Liquid level
- Number of phases
- Phase composition
- Size, location and orientation of the hole
- Level swell, which influences the mass flow rate significantly

All these factors, except level swell, were considered in the simulations reported in this thesis.

2.3 Fluid flow models

The prediction of the flow rate in case of an accidental leak from a pressurized vessel is a dynamic problem. As the fluid is released, the vessel undergoes depressurization and the vessel fluid expands with a change in its properties as well as

possible phase change. The study of the pressurized releases has generated significant research interest in the past, leading to the development of several fluid flow models that predict discharge rates. Such models require the development of the mass and energy balances, phase changes calculation and the evaluation of several thermodynamic properties, which is a particularly tedious process.

There are two different classes of models for two phase flow across orifices (Giacchetta, Leporini, Marchetti, & Terenzi, 2014): Homogeneous and Non-homogeneous models. Homogeneous models consider the mixture as single fluid and that the thermodynamic and physical properties can be obtained by averaging phase properties. They also assume the same speed for all phases. However, Non-homogeneous models consider these assumptions as invalid. Various models are discussed in the following sections and the main difference between them is whether the residence time is long enough to allow stream to flash to equilibrium saturation condition as the pressure falls along the flow path (Huff, 1993).

Homogeneous class of models can be further divided into:

- Equilibrium models – These set of models assume a thermodynamic equilibrium between phase. Eg: Homogeneous Equilibrium Model (HEM);
- Non-Equilibrium models - The non-equilibrium effects are due to phase change process delay with respect to fast fluid transition. Eg: Homogeneous Frozen Model (HFM)

2.3.1 Equilibrium models

Homogeneous Equilibrium Model

The most simple model is the Homogeneous Equilibrium Model (HEM). It assumes that the phases are in thermodynamic equilibrium with each other and their equal average speeds can be utilized. Also, fluid expansion is considered as isentropic (Lenclud & Venart, 1996). In this model, the flow is called choked, when the value of mass flux is maximum for a given set of stagnation properties:

$$G_c = \max\left(-\frac{1}{v_{ex}}[2(h_{fluid} - h_{ex})]^{\frac{1}{2}}\right) \quad (1)$$

where,

G_c = Critical mass flux

v_{ex} = Specific of the fluid at the exit throat

h_{fluid} = Enthalpy per unit mass of the fluid

h_{ex} = Enthalpy per unit mass of the fluid at the exit throat

The HEM was extensively developed by Leung and Leung et al. Leung et al. (1986, 1990b) used the key concept of equation of state for two-phase specific volume and proposed an approximate equation of state for HEM based on stagnation conditions (Fthenakis, 1993). Leung (1989) developed a unified approach for compressible flow of two-phase mixtures through nozzles and pipes. His approach accounts for the effects due to friction, gravitational change, inlet sub-cooling and presence of non-condensable gases (Leung, 1990).

Omega method

Leung (1995) proposed Omega method that accounts for the compressibility of the two-phase mixture in the HEM. It is the most common method used for calculating the mass flow rate for a gas/liquid two phase flow. This method is adopted and recommended by The American Petroleum Institute because of its conservative results. It is based on the homogeneous flow model in which both gas and liquid are at same velocity and are uniformly distributed across the flow cross section, and both the phases are in equilibrium with each other (Giacchetta et al., 2014). However, these assumptions are only valid in the case of the spray or wet vapor flow, where there are only a few drops of liquid in the vapor. Later Diener (2005) showed that the Omega method is unsuitable for inlet flow conditions involving boiling liquids with only low vapor contents.

Raimondi's method

Raimondi (2007) identified that the Omega method used by API cannot be applicable to multicomponent systems at high pressure where retrograde condensation and evaporation may appear. Omega method introduces different calculation procedures for different discharged systems. Fluid systems are classified as flashing or non-flashing systems containing condensable or non-condensable components. This makes it difficult to apply in complex cases and near thermodynamic critical point. The recent extension of Omega method by Deiner-Schmidt does not resolve these problems. He proposes a rigorous and unified approach for the calculation of critical flow conditions through nozzle for multicomponent and multiphase mixtures. His study proposes an algorithm

for calculation of maximum allowable flow rate discharged through an orifice for given upstream conditions. It is based on the evaluation of sonic velocity using the equation of state that are used for calculation of thermodynamic properties (L. Raimondi, 2007).

Moody's model

Moody (1965) proposed an alternative model that assumes annular flow, uniform linear velocities of each phase (but not equal) and equilibrium between liquid and vapor phase. This model predicts maximum flow rate of a single component, two-phase mixture. The flow rate is maximum when it's derivative with respect to the exit slip ratio (velocity ratio) and the exit pressure are equal to zero (Lenclud & Venart, 1996).

Nielsen's model

Nielsen (1991) presented a model that predicts the release rate of superheated liquids from a vessel to the surroundings via a pipe. The model was derived by assuming a frozen situation such that both flashing and non-flashing zone coexist in the pipe. For the flashing zone, it was assumed that the mixture of liquid and vapor are homogeneous, expansion is isenthalpic and there is thermodynamic equilibrium between the phases. The main purpose of this study was to assess the conditions for which the homogeneous equilibrium model can accurately predict mass flow rates. The model results were compared with experimental results of a release of superheated water from a tank via a 2m long pipe. The study indicated that under critical two-phase flow conditions, the mass flux can be predicted with good accuracy for materials other than water, provided that the liquid viscosity at boiling point temperature, Tb is close to or less than that of water at 100C, the pipe diameter$\geq$ 0.01 m and $3 \leq L/D \leq 175$F. It was concluded that

HEM gives a maximum error of -10% due to model deficiencies under the above conditions (Nielsen, 1991).

Norris and Puls

Norris and Puls (1993a) proposed a mechanistic model for simulating single and multiphase flows. The model assumes a homogeneous thermodynamic equilibrium. In this model, the fluid phase behavior and the fluid properties are calculated using an equation of state model that carries out either isothermal or isentropic flashes over a range of pressures. This model was tested in 1993 for hydrocarbon blowdown from vessels and pipelines (Norris & Puls, 1993b). However, the proposed model was unable to predict the vessel fluid temperature variations, did not account for momentum and energy balance, and gravity segregation (Norris & Puls, 1993a, 1993b). Some of the simulations carried out in these papers were repeated for validation of the code developed in this thesis.

Cumber's model

Cumber (2001) developed an outflow model to predict mass flow rates of releases from high pressure vessels accurately in a fast and robust manner. The model developed assumes a single control volume, no heat transfer as its effect on the mass flow rate is small during initial stages of discharge when the flow rate is the highest. The Peng-Robinson equation of state (EOS) was used. Also, thermodynamic equilibrium between two phases is assumed. However, when rapid depressurization occurs, non-equilibrium effects may have small influence on the mass flow rate. Upon testing, the model predicted the pressure and flow rate reasonably accurately for a vessel with gas

phase content. However, some of the assumptions were found to be invalid, such as, adiabatic vessel wall assumption. This assumption was based on the fact that, in early stages of depressurization, the heat transfer is less. However, in latter stages heat transfer to the vessel changes vessel temperature which has second order effect on the mass flow rate. Additionally, this assumption tends to under predict the vessel temperature and slightly over predict the mass flow rate (Cumber, 2001).

2.3.2 Non-equilibrium models

Homogeneous Frozen Model

One of the important Non-equilibrium models is the Homogeneous Frozen Model (HFM) (Lenclud & Venart, 1996). This model describes the flow of a nonvolatile liquid phase and an insoluble gas phase (Huff, 1993). This model assumes that:

- Two phase velocities are equal
- No mass transfer between the two phases during the efflux
- Wall shear forces can be neglected
- Liquid is incompressible
- Isentropic expansion of vapor

The critical mass flux can be written as:

$$G_c = \sqrt{\frac{\gamma P}{x v_g} (\eta)^{(1+\gamma)/\gamma}} \qquad (2)$$

where,

γ = Isentropic exponent or heat capacity ratio

P = Pressure

x = Quality

v_g = Specific volume of the gas

η = Critical pressure ratio

Henry-Fauske's model

This model forms the basis of a family of models that describe varying extents of non-equilibrium behavior. It presumes a non-equilibrium homogeneous flow. Hence, it is also called as the Homogeneous Non-Equilibrium Model (HNE). This model also describes the behavior of fluids which are subcooled at inlet pressure, but reach saturation conditions within the nozzle (Huff, 1993). It is recommended in case of short nozzles and orifices, where the residence time of the mixture is too short for significant evaporation. This model assumes that:

- No heat or mass transfer occurs in the nozzle. However, mass and heat transfer rates between the phases at the throat are not negligible
- The two phases have same velocity
- Gas expands isentropically and liquid is incompressible
- At the throat, the vapor behaves polytropically and is not in equilibrium

Equilibrium Rate Model

Fauske (1985) and Grolmes (1990) derived a simple extension of the HEM that was termed as Fauske's equilibrium rate model. Fauske introduced a non-equilibrium

term N to the orifice equation, to define the Equilibrium Rate Model (ERM) flux (Fthenakis, 1993):

$$G_{ERM}^2 = \frac{G_{CL}^2}{N} \tag{3}$$

$$N = 10L + \frac{G_{CL}^2}{C_0^2 G_L^2} \tag{4}$$

where,

G_{ERM} = Equilibrium rate model flux

G_{CL} = Critical mass flux with low inlet quality

G_L = Mass flux of all-liquid flow

C_0 = Discharge coefficient

Homogeneous Non-Equilibrium method by Diener and Schmidt

Diener and Schmidt (2005) proposed an extension to the omega method by adding an equation for boiling delay coefficient that accounts for the boiling delay. This method called the Homogeneous Non-Equilibrium method by Diener and Schmidt (HNE-DS) accounts for the boiling delay, hydrodynamics non-equilibrium and calculates reliably the flow rate in both flashing and non-flashing flow (Diener & Schmidt, 2005).

According to Whalley (Whalley, 1987), HEM when compared to experimental data gives a good critical pressure ratio. Critical pressure ratio is a ratio of critical pressure at choked plane to the initial pressure (Semantic Globe Thermal Sciences, 2010). However, it underestimates the flow rate. On the other hand, HFM, predicts the

flow rate well and underestimates the critical pressure ratio. Moody's model overestimates the flow rate. The empirical Henry-Fauske's model is the most promising one according to Lenclud and Venart (1996).

2.4 Computer programs

Models for leaks from pressurized vessel form the backbone of computer programs developed overtime for the industry. Some of them are discussed in this sub-section.

2.4.1 LEKCON

Woodward et al. (1990) proposed a computer program following Fauske's equilibrium rate model for sonic releases. LEAKR, developed for the Environment of Canada, calculates single or two phase discharge rates. Also, it uses mass release instead of volume release increments. This was later extended using technology from DIERS (Design Institute of Emergency Relief Systems) and DIPPR (Design Institute of Physical Properties Research) to form LEAKER that calculates discharge rates from vessels. In 1989, LEAKER and other programs were integrated to produce a single tool to predict the effects of an accidental release from a process vessel. This program was called as LEKCON (Woodward, 1990). Table 1 lists the computer programs that were integrated to form LEKCON.

The program proposed accounted for various geometries: horizontal, vertical and spherical cylinders. The vessel could be placed at an elevation or on ground, and insulated/partly-insulated or uninsulated. The program also accounted for the

relationship between height of puncture and liquid level, as this decides the release phase (Woodward, 1990).

Table 1: Computer programs that were integrated to form LEKCON (Woodward, 1990)

Computer Programs	**Function**
DIPPR	Sets up physical properties file
SETUP	Interactive program to build input files
LEAKER	Calculates discharge rates from vessels
LPOOL	Calculates pool spread and vaporization
JETLEK	Calculates dispersion for elevated, high-momentum releases
DEGADIS-PC	Calculates dispersion for ground level releases of aerosol or heavy vapor

2.4.2 BLOWDOWN

BLOWDOWN was initially developed at Imperial College to predict vessel wall temperatures and prevent brittle failures. It was used for simulation of depressurization of networks of vessels and associated pipework on offshore oil and gas platforms. It was later extended for simulation of depressurization of pipelines. Some of the main features of the program are as follows (Richardson & Saville, 1996):

- It does not assume thermodynamic equilibrium and can have up to three phases
- The pressure, temperature, density dependency is modelled using an equation of state based on an extended corresponding state principle, which is more accurate than the cubic equation of state. However, it requires more run-time
- Pipelines are divided axially such that changes in physical properties along the element may be neglected
- Vessels are divided into three zones: i) Top zone of gaseous hydrocarbon ii) Middle zone of liquid hydrocarbon iii) Bottom zone of free water
- Depressurization is broken down into a sequence of pressure instead of time, as pressure is a more important parameter thermodynamically
- Flow is assumed to be quasi-steady irrespective of being single phase or two-phase. Also, if it is two-phase, then it has to be homogeneous.

2.4.3 SAFIRE

SAFIRE is also a vessel depressurization model developed for vent sizing pressure vessels used for batch processing chemicals where runaway chemical reactions occur. Some of its features are as follows (Cumber, 2001):

- The vessel is modelled as a single control volume
- Thermodynamic equilibrium is assumed
- Numerical robustness has been found to be a problem

2.4.4 OLGA

Bendelksen et al. (1991) presented OLGA, a dynamic two-fluid program for simulation of two phase oil and gas flows in pipelines. The first version of OLGA was developed in 1983. However, it was later extended and further developed for a research program between Institute of Energy and Technology and SINTEF (The Foundation for Scientific and Industrial Research, Scandinavia). The empirical basis of the model was extended and new applications were introduced. The program could make accurate predictions of pressure drop, liquid hold-up and flow-regime transitions. Flow-regimes were now treated as an integral part of the two-fluid system. OLGA was tested against experimental data from SINTEF two-phase flow laboratory and from literature. Predictions were in good agreement with the data from literature and experiments (Bendlk, Maine, Moe, Nuland, & Technology, 1991).

OLGA as of now implements a one dimensional model for three phase hydrocarbon flow in pipelines and pipeline networks. This model consists of separate continuity equations for gas, liquid bulk and liquid droplets that may be coupled through interfacial mass transfer (Giacchetta et al., 2014).

2.4.5 RELEASE

In 1999, RELEASE was developed to simulate continuous steady state flow of a liquid discharge from an orifice with no reaction and subsequent near field entrainment and jet spreading. It can predict the rate of fluid discharge, depressurization, flashing and formation of liquid drops, entrainment of drops into vapor cloud, subsequent jet

spreading and rate of liquid rainout to a pool on the ground (Johnson & Woodward, 1999).

2.4.6 PHAST

PHAST, a consequence modelling package developed by DNV, includes models for discharge of hazardous chemicals to the atmosphere. For pressurized releases from vessels/pipes, the final part of PHAST discharge model is the 'flash model' which calculates depressurization from the exit pressure to ambient pressure (Witlox, 2002).

2.4.7 BLOWSIM

From 1999 to 2007, Mahgerefteh et al. developed mathematical models for simulation of accidental leaks and predicting the outflow. Mahgerefteh developed a procedure based on the method of characteristics (Mahgerefteh, Saha, & Economou, 2000). Mahgerefteh & Wong (1999) developed a model, termed as BLOWSIM that incorporated cubic equation of states. BLOWSIM also accounted for heat transfer effects, inter-phase fluxes and effects of sonic flow. Mahgerefteh et al. (2002) developed a numerical simulation method for predicting the blowdown of high-pressure cylindrical vessels under a fire attack. This was developed by incorporating transient thermal and pressure stress effects into the BLOWSIM model. This model accounts for non-equilibrium effects between phases, heat transfer between fluid phases and their corresponding sections of the vessel wall, interphase fluxes due to evaporation and condensation, and the effects of sonic flow at the orifice.

2.5 Procedures used in the simulation of this work

The aim of this thesis work is to develop a model that describes the dynamics of a fluid leaking from a pressurized vessel. The code developed is an integration of two other algorithm previously developed by Castier – 1) isochoric-isoenergetic (UVN) flash (Castier, 2009) and 2) sound speed calculations in multiphase systems (Castier, 2011).

2.5.1 Development of UVN flash

Saha and Caroll (1997) proposed an isoenergetic and isochoric (UVN) flash method to simulate the dynamic filling of a process vessel. Unlike many other flashes, in this case, neither pressure nor temperature is known. This paper discusses a scheme for solving the dynamic tank problem, wherein mass and energy balances are solved first and then the equilibrium at each time step. The phase equilibrium was solved using an algorithm with nested loops (Saha & Carroll, 1997).

Michelson (1999) suggested in his paper to investigate UVN flashes with direct iterations in temperature, phase volumes and moles numbers of each component in each phase, using the Hemholtz energy as a core function (Michelsen, 1999). Goncalves et. al used this suggestion and proposed a single loop approach with direct iterations in phase volumes for solving algebraic equations. It was later found that this iterative procedure becomes unreliable close to saturation points and a new alternative was proposed(Goncalves, Castier, & Araujo, 2007).

Castier (2010) developed an algorithm that solves UVN flash problems by direct entropy maximization in a single loop. This flash procedure calculates the conditions of the fluid in the tank and takes into account phase appearance and disappearance and also

is fit for solving two and three phase equilibrium problems (Castier, 2010). This algorithm was integrated with a dynamic simulator designed to handle pre-defined leak flow rates. However, the focus of this thesis is on the dynamics of vessels in which the flow rate changes overtime as a result of pressure differences between the vessel and the environment.

2.5.2 Variable flow rate

To have a variable flow rate, a UVN flash algorithm was integrated with an algorithm to calculate the sound speed of the fluid at the leak location. Details of this integration are discussed in Section 4. It is necessary to characterize the flow regime choked or non-choked. It should be observed that at the exit location, the leaking fluid may have more than one phase. For this reason, a multiphase sound speed procedure is used (Castier, 2011).

A lot of literature work has been done in the area of accidental fluid releases. The literature search showed a good number of models and programs that were developed for leaks from vessels, pipes, nozzles and orifices. These models calculate the discharge rates, predict pressure and temperature variations, and perform a consequence analysis. However, the focus of these models is around the leaking region. There are very few models that simulate dynamics of fluid within vessels. Only a few models account for different vessel and hole geometries; and the relationship between position of leak and the leaking phase. This work proposes a single approach that simulates the dynamics of the fluid within the vessel and couples it with the fluid behavior as it goes through the nozzle (leaking region). The procedure presented uses a single thermodynamic model for

all of the calculations. It is a rigorous simulation method for accidental releases, wherein, the conditions of fluid within the vessel, the fluid properties at the leak point and the leak flow rate are calculated at regular time intervals. The calculation of leak flow rate accounts for the phenomena of choked and non-choked flows. This work considers the relationship between the leaking phase and the level of liquid-vapor interface. It believes that the vessel and hole geometries make a difference to the liquid-vapor interface. The calculation of thermodynamic properties of the fluid and the leak flow rate are carried out using flash calculations with nested loops and involve several iterations to ensure the accuracy of the results. The features of this code have never been seen together in any of the methods proposed before.

3. SCOPE OF WORK

The aim of this thesis was to develop a computational procedure to simulate the dynamics of an accidental leak from a vessel in which the flow rate changes over time. Many of the reviewed papers use the ideal gas equation of state. However, this work does not, and accounts for non-ideal fluid behavior by using the Peng-Robinson (Peng & Robinson, 1976) EOS. This thermodynamic model is widely used for chemical process design, especially in the oil, gas, and petrochemical industries. Using the ideal gas equation of state has the advantage of simplicity because many of the physical property expressions are simple but limits the dynamic model to low pressure applications. With a cubic equation of state, such as the Peng-Robinson model, the expressions for the evaluation of physical properties are more complicated but provide predictions that are more accurate. Moreover, unlike the ideal gas equation of state, the Peng-Robinson model allows the prediction of liquid and vapor phase properties. Therefore, the model for the dynamic behavior of fluids in vessels can account for the existence of liquid and vapor phases either inside the tank or at the exit point, where the fluid leaves the tank.

Prior to this thesis work, Castier had developed a program to simulate the dynamics of accidental vessel leaks wherein the discharge flow rate remains fixed (Castier, 2010). The formulation leads to a system of differential algebraic equations. The differential equations are the component mass balances and the energy (U) balance. It is assumed that the vessel is rigid, i.e., its volume (V) does not change during the leaking period. The numerical integration of the differential mass and energy balances

give, at each moment in time, the values of internal energy and mole numbers of each component in the tank (N). Thus, with known values of UVN, the values of the other thermodynamic properties can be found by solving a UVN flash problem. Castier (Castier, 2009) developed an algorithm to solve this problem based on maximizing the system's entropy using a single iterative loop, backed by a nested-loop iterative procedure for the rare cases in which the single loop approach fails to converge.

The program that Castier (2010) developed to simulate the dynamics of accidental leaks was improved in this thesis to account for the following:

a) Different geometry of tank

b) Different geometry of hole

c) Position of leak

d) Variable leak flow rates

The following possible geometries for the tank were considered: spherical, vertical cylinder, horizontal cylinder, and horizontal cylinder with hemispherical caps. Tank geometry matters because, for example, if a tank has liquid and vapor phases inside it, the leaking of a certain amount of material displaces the position of the vapor-liquid interface differently, depending on tank shape and dimensions. The geometry of the hole also matters and two possibilities were considered: circular and rectangular holes. The latter is useful if, for example, one needs to simulate the effect of a longitudinal crack in the vessel wall. The position of the leaking point is important because, if it is below a vapor-liquid interface, the leak will be from the liquid phase. If

it is above, the vapor phase will leak, under the assumption, adopted in this work, that there will be no surge in the level of the interface because of disorderly vaporization.

The most complex contribution of this thesis was to include the possibility of variable flow rates. To accomplish that, it is necessary to decide whether the leaking flow is choked or not, i.e., at sonic or subsonic speed at the exit point. Thus, it was decided to integrate sound speed calculations into this algorithm. However, the leaking fluid may have one or more phases at the point of leak. If it has more than one phase, a specific algorithm for sound speed in multiphase systems needs to be used. The adopted procedure uses an algorithm developed by Castier (2011) for this purpose. The sound speed algorithm calculates the sound speed of the fluid at the exit of the leak assuming the leaking point is the throat of a hypothetical adiabatic converging nozzle that operates isentropically. The fluid at the entrance of this hypothetical nozzle is assumed to have negligible velocity (supposed equal to zero) and the thermodynamic properties of the leaking phase. At the exit point, it has non-zero velocity, determined by solving the energy balance and the isentropic condition. If the calculated velocity is higher than the sound speed at the given conditions, this solution has to be rejected because the flow would be supersonic, something that cannot happen at the exit of this hypothetical converging nozzle. In this case, the energy balance and isentropic conditions are solved again, imposing that the flow will be sonic at the exit point from the vessel. The results of this sequence of steps define whether the flow is choked or non-choked.

4. METHODOLOGY

This section describes the computational procedure developed for the dynamic simulation of leaks. As the procedure involves many steps, the presentation begins with a description of how these steps are interconnected. Then, a description of each follows. This section ends with comments about the importance of accurate initial estimates for the several iterative calculations that are carried out and about the numerical difficulties faced during the course of this project.

Figure 1 shows the flow of calculations in the code developed. The first step to simulate an accidental vessel leak is to define the system in terms of tank geometry (shape and dimensions, from which its volume can be computed), initial temperature and number of moles of each component, and characterizing properties of the fluid within the tank. In this work, these properties are the critical temperature, critical pressure, and acentric factor of each component, their binary interaction parameters for the Peng-Robinson equation of state, and the coefficients of a polynomial expression for the molar heat capacity at constant pressure in the ideal gas state. With these specified values of temperature, volume, and component amounts, the state of the fluid in the tank can be determined by minimizing the system's Helmholtz energy, i.e., by solving a so-called TVN flash problem. An algorithm proposed by Espósito et al. (Esposito, Castier, & Tavares, 2000) is used, thereby finding the number of phases present, their volumes, the amount of each component in each phase, and the internal energy of the fluid.

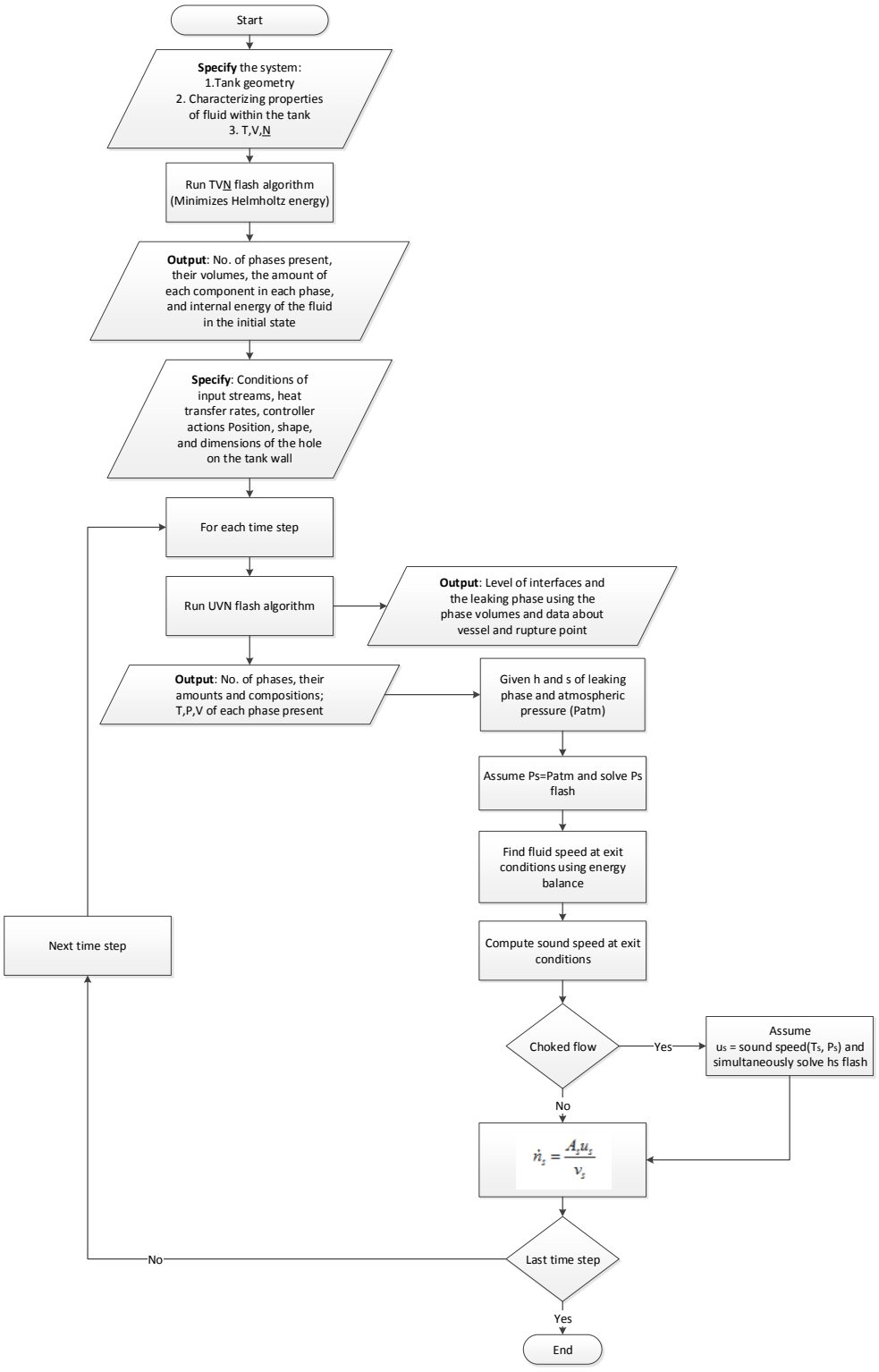

Figure 1: Flow of calculations in the code developed

The next step is to specify variables that define the dynamics of the leaking process. They include the conditions of input streams to the tank, heat transfer rates to or from the tank, and controller actions, all of which the computational procedure can handle. In the examples of this thesis, all these effects are considered as absent because of the focus on simple leaking processes. Another set of variables associated with the dynamic process includes the position, shape, and dimensions of the hole on the tank wall, from which the leaking rate can be computed.

The final step is to execute the dynamic simulations using a Fortran program that combines several algorithms. The key computation of these simulations is the numerical integration of the mass and energy balances in the vessel, allowing the evaluation of the internal energy and component amounts of the fluid in the tank at each moment in time. At each time step during this numerical integration, the following computations take place:

a) Solution of a UVN flash problem to determine the state of the fluid in the vessel. This provides information about the number of phases, their amounts and compositions, the temperature, the pressure, and the volume of each phase present;
b) Determination of the level of the interfaces, if more than one phase is present, using the phase volumes and data about the vessel shape and size. Combining this with information about the rupture point (position, shape, and size), it is possible to determine the leaking phase(s).

c) Determination of the leak flow rate, based on the following assumptions: (i) the region inside the vessel next to the leaking point forms a hypothetical steady-state converging nozzle; (ii) this nozzle's operation is adiabatic and isentropic; (iii) the velocity of the fluid inside the vessel is negligible; (iv) the velocity of the fluid at the exit point is different from zero; (v) the exiting fluid may have more than one phase. The mass and energy balances and the isentropic condition in the nozzle, under the assumption that the fluid leaves at atmospheric pressure, constitute a flash problem whose solution gives the number of phases, their amounts, volumes, densities, and temperature. Combining these data with the leak area, it is possible to find the fluid velocity at the exit point.

d) Verification of choking or non-choking flow conditions. The sound speed at the conditions of the exit point is determined and compared to the fluid velocity computed in item 3. If the flow is subsonic, its conditions are passed to the numerical integrator of the mass and energy balances in the vessel for the calculations of the next time step. However, if the flow is supersonic, the results are discarded because the maximum allowable fluid velocity at the exit point of this nozzle is the sound speed. Then, the calculation outlined in item (c) is repeated, imposing that the exit flow will be at sonic speed and relaxing the exit pressure specification, i.e., it becomes a calculated value. The conditions are then passed to the numerical integrator of the mass and energy balances in the vessel.

The following sections discuss these steps in detail.

4.1 System

The simulated system consists of a fluid leaking from a vessel (Figure 2). The main modelling assumptions are:

- The fluid in the tank is in equilibrium at all times;
- No chemical reaction occurs;
- The vessel volume is known and fixed;
- The leak occurs through a hole at a known vertical position;
- The size of the hole remains constant;
- The leaking area behaves as a hypothetical adiabatic converging nozzle that operates isentropically (Figure 3).

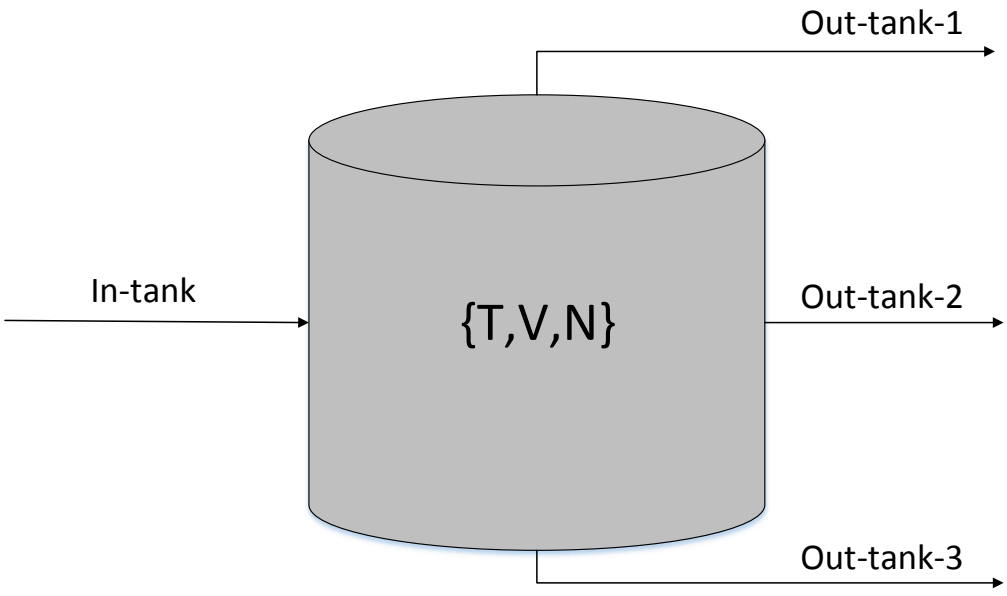

Figure 2: A simple vessel with input and output streams

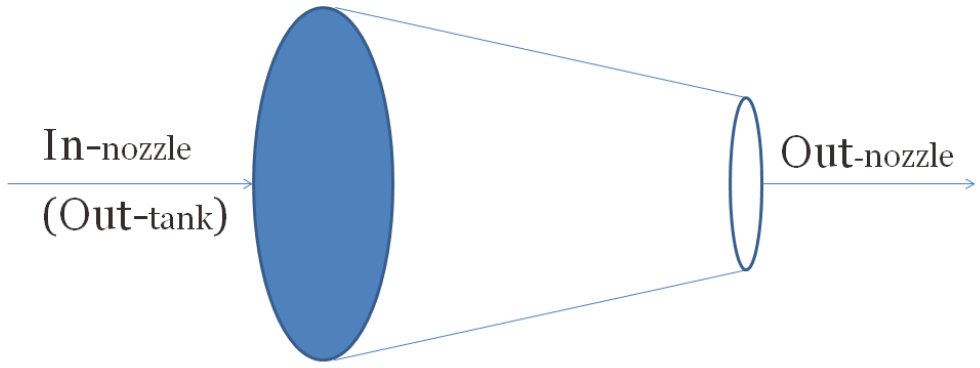

Figure 3: Converging nozzle (leaking point) with input and output streams

4.2 Vessel and hole geometries

The code developed in this thesis accounts for different vessel and hole geometries. Figure 4 shows the possible vessel geometries considered, which were: (a) vertical cylinder, (b) horizontal cylinder, (c) horizontal cylinder with hemispherical caps, and (d) spherical cylinder. The vessel diameter (ϕ) is a specification in all cases and the length of the cylindrical section (L) is also a specification, with exception of the spherical vessel. If the vessel contains a liquid and vapor phase, in the event of a leak, the position of liquid-vapor interface depends on the volume of each phase, tank shape and dimensions.

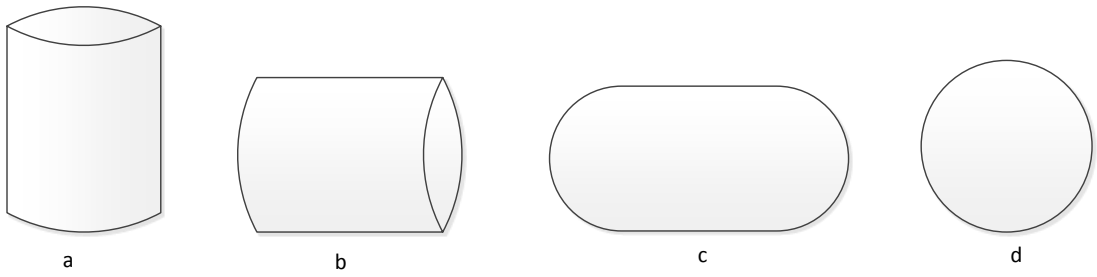

Figure 4: (a) Vertical cylinder; (b) Horizontal cylinder; (c) Horizontal cylinder with hemispherical caps; (d) Spherical vessel

For the hole, spherical and rectangular geometries were considered. Figure 5 shows these two types of ruptures.

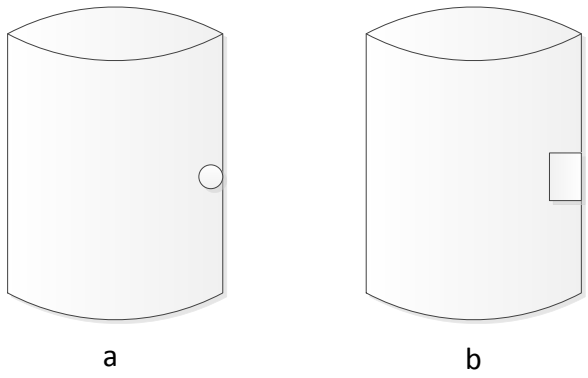

Figure 5: a) Tank with circular rupture; b) Tank with rectangular rupture

4.3 Position of the rupture decides the leaking phase

Another feature added to the code is the relation between leaking phase and the position of the rupture. From Figure 6, it can be seen that:

- In case (a), the fluid leaking is liquid (2)

- In case (b), the fluid leaking is a mixture of both liquid (2) and vapor (1)
- In case (c), the fluid leaking is vapor (1)

Figure 6 shows how the position of the rupture decides the leaking phase of the fluid.

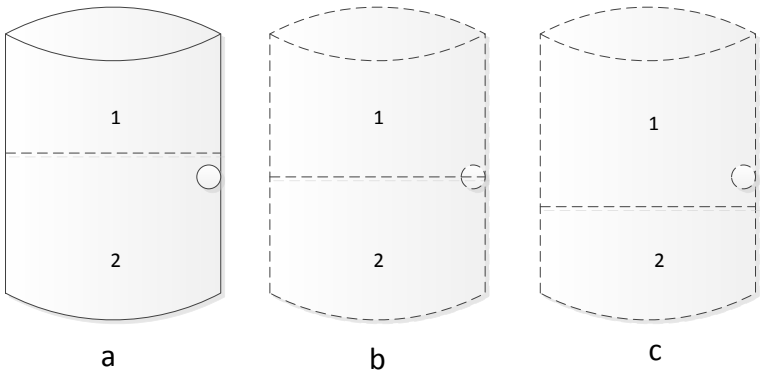

Figure 6: Different phase leaks based on position of hole

The most intuitive way of determining the leaking phase is to compare the level of the interface to the position of the rupture. However, phase volumes are direct outcomes of the UVN flash problem that determines the state of the fluid inside the vessel. Conversion of the phase volumes to interface levels is simple for a vertical cylinder but may even involve iterative procedures for other vessel geometries, as discussed later.

A generalized procedure has been implemented and is applicable to any number of phases and rupture points, with any combination of the tank and hole geometries presented in the previous section. For the sake of simplicity, its conceptual development

is explained for the case of two phases and a single rupture point in a vertical cylindrical vessel. In Figure 7, points h_{rl} and h_{rh} denote the vertical positions of the lower and upper limits of the rupture, both measured from the bottom of the vessel. The next step is to compute V_{rl} and V_{rh}, which are the volumes measured from the bottom of the tank up to each of these vertical positions. Note that V_{rl} and V_{rh} only depend on geometric quantities and it sufficient to compute them once, at the beginning of a given simulation.

A comparison of volumes allows the identification of the leaking phase(s). If $V_2 \geq V_{rh}$ (case (a) in Figure 6), the leak is from the liquid phase; if $V_2 \leq V_{rl}$ (case (c) in Figure 6), the leak is from the vapor phase; and if $V_{rh} < V_2 < V_{rl}$, the liquid and vapor phases leak simultaneously. In the latter case, the molar composition of leaking fluid is estimated as a linear combination of the mole fractions in each phase, weighted according to the fraction of the hole area that is exposed to each phase. The underlying assumption is that the liquid and vapor phases inside the tank move toward the leaking hole with equal speeds. To make this calculation, it is necessary to find the exact level of the interface in order to evaluate the hole area fractions. Here, consider that h is the position of the interface. Details about its evaluation will be presented later.

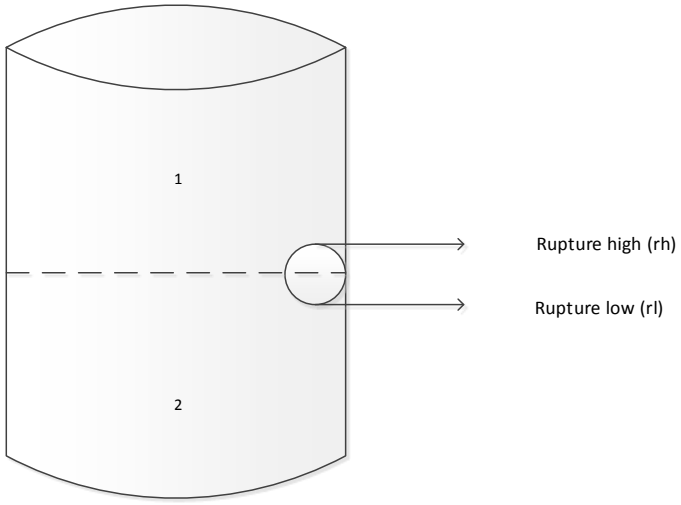

Figure 7: Cylindrical vessel showing high and low end levels of rupture

For a rectangular rupture of width b, the areas exposed to phases 1 and 2 are equal to:

$$A_1 = b\left(h_{rh} - h\right) \tag{5}$$

$$A_2 = b\left(h - h_{rl}\right) \tag{6}$$

For a circular rupture, the evaluation of the areas exposed to phases 1 and 2 involves several steps. In the discussion that follows, r_c denotes the radius of the circular hole. To compute the area exposed to phase 1, assign $C = h_{rh} - h$ and find:

$$A_1 = r_c^2 cos^{-1}\left(\frac{r_c - C}{r_c}\right) - (r_c - C)\sqrt{2r_c C - C^2} \tag{7}$$

To compute the area exposed to phase 2, the same procedure is followed, with the assignment $C = h - h_{rl}$, leading to a formula analogous to that for A_1.

To apply these formulae, it is necessary to know the height of the interface (h), whose evaluation depends on the vessel geometry as summarized in Table 2. For a vertical cylinder, the formulae are straightforward. However, for horizontal cylinder, horizontal cylinder with hemispherical caps and spherical tanks, finding the level involves iterative calculations whose goal is to find the zero of each function f shown in Table 2. This was carried out using the Newton-Raphson method and the derivative of each of these functions with respect with the height appears in Table 2. These calculations were assumed to converge when the absolute value of the relative deviation of the height value in consecutive iterations was less than 10^{-8}. Figures 8, 9 and 10 show how, for each of these geometries, the cross sectional area of the fluid varies along the height of the vessel. In the computational program, the implementation was developed for any number of phases, but for simplicity, the presentation here is limited to only two, a liquid and vapor phase.

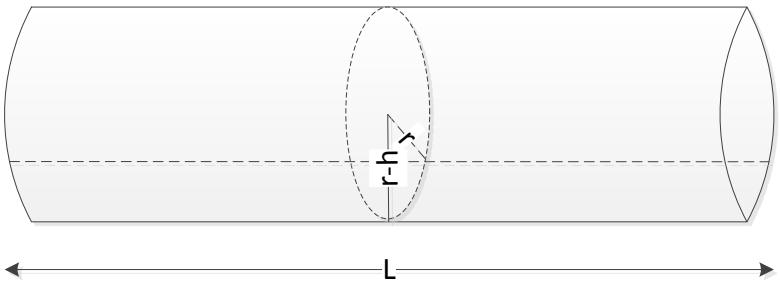

Figure 8: Changing cross sectional area with fluid level: Horizontal cylinder

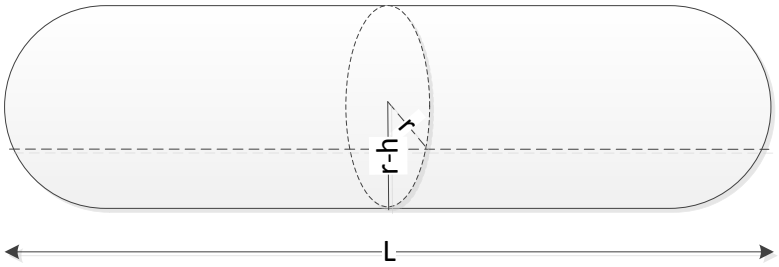

Figure 9: Changing cross sectional area with fluid level: Horizontal cylinder with hemispherical caps

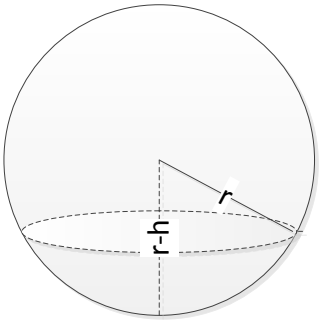

Figure 10: Changing cross sectional area with fluid level: Spherical vessel

In Table 2, d and r are the diameter and radius of the vessel, respectively, and h and V are the height and volume of liquid in the vessel.

Table 2: Equations of Area and height for different geometries of tank and hole

Tank/Hole	Area and Height
Vertical Cylinder	$A=\frac{\pi d^2}{4}$ (8) $h=\frac{V}{A}$ (9)
Horizontal Cylinder	$f = -\frac{V}{L}-(r-h)\sqrt{2hr-h^2}+ r^2cos^{-1}(\frac{r-h}{r})$ (10) $\frac{df}{dh}=\frac{-\left((r-h)(2r-2h)\right)}{2\sqrt{2hr- h^2}}+\sqrt{2hr-h^2}+\frac{r}{\sqrt{1-\frac{(r-h)^2}{r^2}}}$ (11)
Horizontal cylinder with hemispherical caps	$f =$ $\frac{\pi h^2(3r-h)}{3}-V+L\left(-\left((r-h)*\sqrt{2hr-h^2}\right)+r^2cos^{-1}\left(\frac{r-h}{r}\right)\right)$ (12) $\frac{df}{dh}=\frac{-\pi h^2}{3}+\frac{2\pi h(3r-h)}{3}+L\left(\frac{-\left((r-h)*\sqrt{2r-2h}\right)}{2\sqrt{2hr-h^2}}+\sqrt{2hr-h^2}+\right.$ $\left.\frac{r}{\sqrt{1-\left(\frac{r-h}{r}\right)^2}}\right)$ (13)
Sphere	$f = h^3-3rh^2+\frac{3V}{\pi}$ (14) $\frac{df}{dh}=3h^2-6rh$ (15)

4.4 Balance equations for the vessel

Mass and energy balance equations can be written for the vessel.

Vessel – Mass Balance

The mass balance equation for each component i is:

$$\frac{\mathrm{dN_i}}{\mathrm{dt}} = \sum_{j=1}^{n_{in}} \dot{n}_{\mathrm{i,j,in-tank}} - \sum_{k=1}^{n_{out}} \dot{n}_{\mathrm{i,k,out-tank}} \tag{16}$$

where,

N_i = Number of moles of component 'i'

$\dot{n}_{\mathrm{i,j,in-tank}}$ = Molar flow rate of 'i' entering the vessel via process stream 'j'

$\dot{n}_{\mathrm{i,k,out-tank}}$ = Molar flow rate of 'i' exiting the vessel via process stream 'k'

Vessel – Energy Balance

$$\frac{\mathrm{dU}}{\mathrm{dt}} = \sum_{j=1}^{n_{in}} \dot{n}_{\mathrm{j,in-tank}}\, \mathrm{h_{j,in-tank}} - \sum_{k=1}^{n_{out}} \dot{n}_{\mathrm{k,out-tank}}\, \mathrm{h_{k,out-tank}} + \dot{Q} \tag{17}$$

where,

U = Total internal energy

$h_{\mathrm{j,in-tank}}$ = Molar enthalpy of stream 'j' entering the vessel

$h_{\mathrm{k,out-tank}}$ = Molar enthalpy of stream 'k' exiting the vessel

$\dot{Q}$ = Heat transfer rate to the vessel

In principle, there are frictional effects when the fluid enters and leaves the tank, which we will neglect.

4.5 Initial state of the fluid - TV<u>N</u> flash algorithm

Dynamic simulations demand knowledge about the initial state of the system. The initial temperature, volume and number of moles are already given and known.

Using the given information, a TVN flash is carried out to find the number of phases, their volumes, amount of each component in each phase and the internal energy. The TVN flash procedure used here adopts the method developed by Esposito et. al (Esposito et al., 2000). The goal of this method is to determine the distribution of the species in the system and the position of phase interface and the internal energy of fluid in initial state.

4.6 Conditions inside the tank - UVN flash algorithm

The system here serves as a good example of an isochoric-isoenergetic flash problem. Castier (2009) had developed an algorithm to solve such a flash problem by direct entropy maximization (Castier, 2009).

Figure 11 shows the general structure of how the UVN flash problem is solved. The basic idea of this algorithm is to maximize the entropy by iterating the values of internal energy, volume and number of moles of each component, for each phase.

In Figure 11, the first test is to check whether a single phase system at the given specification of T and P is feasible. If a single phase configuration occurs with positive values of temperature and pressure, the next step is to test its global stability. If it turns out unstable, a new phase is added and entropy is maximized. During the entropy maximization, the algorithm tests if merging the two phases gives a larger entropy value. If it does, a phase is removed.

However, if the single phase configuration has negative temperature or pressure, the system goes through phase addition. If the pressure is negative, the algorithm finds a temperature that gives a small positive pressure for the single phase system. These new values of temperature and pressure would correspond to the new phase to be added.

Global phase stability tests are used to find initial estimates of molar internal energy, molar volume and mole fractions of the components of the new incipient phase. The amount of the new phase added is taken as equal to 1 x 10^{-10} times the total number of moles, so that the bulk phase is similar to the one phase configuration. Two-phase calculations are then carried out. In this process, the volume of the bulk phase decreases and that of the incipient phase increases until the bulk phase pressure becomes positive. Then the entropy maximization is performed.

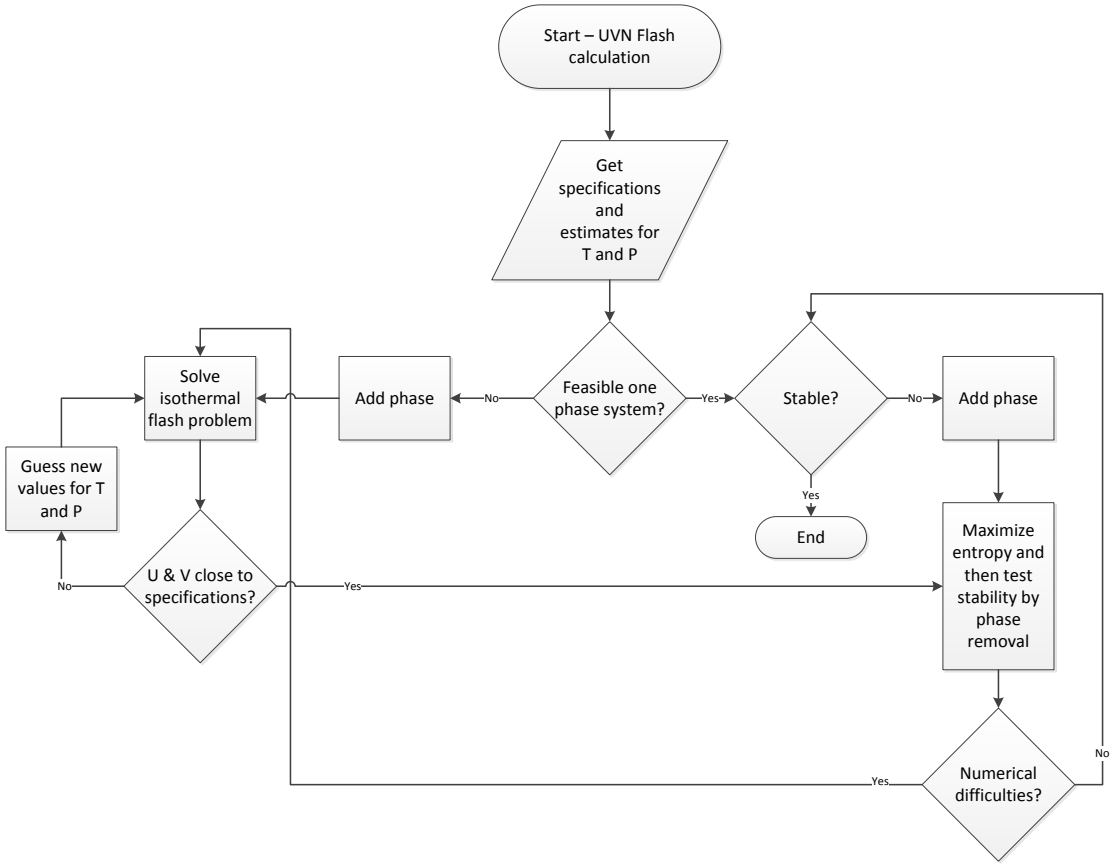

Figure 11: UV<u>N</u> flash algorithm flowchart (Castier, 2009)

However, if the temperature is negative, a nested loop approach is taken in which a TPN flash is solved in the inner loop and, temperature and pressure values are updated in the outer loop. Once a solution is obtained by this approach for the UVN flash, the entropy maximization procedure is activated. The process of entropy maximization may face problems in convergence. However, convergence of entropy maximization in dynamic solution should be easier because the converged values at each time step serve as good estimates for the next.

4.7 Leak flow rates - Sound speed calculations

The code developed for UVN flash could simulate the dynamics of a vessel leak but with the assumption that the leak rate is fixed. To account for a variable flow rate, it was necessary to know if the flow is choked or non-choked, which requires the evaluation of sound speed at the exit conditions. Therefore, sound speed calculations were integrated with the other procedures. Because the leak may be single phase or multiphase, an algorithm developed by Castier (2011) to calculate the thermodynamic sound of speed in system with any number of fluid phases was used. The structure of this integration was shown in Figure 1.

4.7.1 Equations

In the equations that follow, the subscript *t* denotes the properties of the fluid that enters the nozzle from the tank.

The subscript *s* denotes the source term, i.e., the properties of the leaking fluid at the nozzle's exit plane, i.e., as it enters the environment around the tank.

The thermodynamic properties in lower case are molar properties. M_s is the molar mass of the leaking fluid at the nozzle's exit plane. For simplicity, one can assume a basis of 1 mole when analyzing equations (18) and (19), below.

Energy balance for adiabatic steady-state flow:

$$h_t = h_s\left(T_s, P_s\right) + M_s \frac{u_s^2}{2} \tag{18}$$

Adiabatic reversible steady-state flow, i.e., isentropic:

$$s_t = s_s\left(T_s, P_s\right) \tag{19}$$

Two procedures may be necessary to solve these equations and evaluate the flow rate of the leak.

4.7.2 Procedure 1

Assume P_s to be known, generally equal to the atmospheric pressure. If the system has a single phase, Eq. (19) can be used to find T_s and then Eq. (18) can be used to find u_s. The problem with this simple approach is that it assumes the fluid has a single phase at the nozzle's exit plane. However, it is possible (at least in principle) that the fluid becomes saturated at the nozzle's exit plane and has more than one phase. Therefore, the general procedure requires the solution of a flash problem with unusual specifications: entropy and enthalpy. The most straightforward way of solving this unusual problem (which takes full advantage of programs we already have) is as follows.

Given P_s (a fixed value), guess values for T_s and u_s. Use Eq. (18) to find the corresponding value of h_s. Using $\{P_s, T_s\}$, solve an isothermal flash problem (already implemented and available). Check whether the calculated values of h_t and s_t match the specification. If they don't, new estimates for T_s and u_s are necessary (generated by some numerical method) until convergence. Figure 12 is a flowchart of these calculations.

Once the problem is solved, it is necessary to compare u_s and the sound speed computed at the converged values of $\{P_s, T_s\}$ (denoted here as $c_s(T_s, P_s)$). Note that the sound speed calculation will use the same thermodynamic model employed for the flash calculation in such a way that all computations are self-consistent, including the possibility of multiple phases at the nozzle's exit plane.

If $u_s \leq c_s$, the flow is subsonic. The molar flow rate will be:

$$\dot{n}_s = \frac{A_s u_s}{v_s} \tag{20}$$

where A_s is the cross-sectional area and v_s is the molar volume of the mixture, both at the nozzle's exit plane. In multiphase flows, v_s incorporates is a weighted average of the molar volumes of all phases (with the assumption that all move at the same speed in the nozzle, consistently with the no hold-up assumption).

If $u_s > c_s$, the solution is not acceptable because a fluid cannot accelerate beyond sonic speed in a converging nozzle. Procedure 2 needs to be activated.

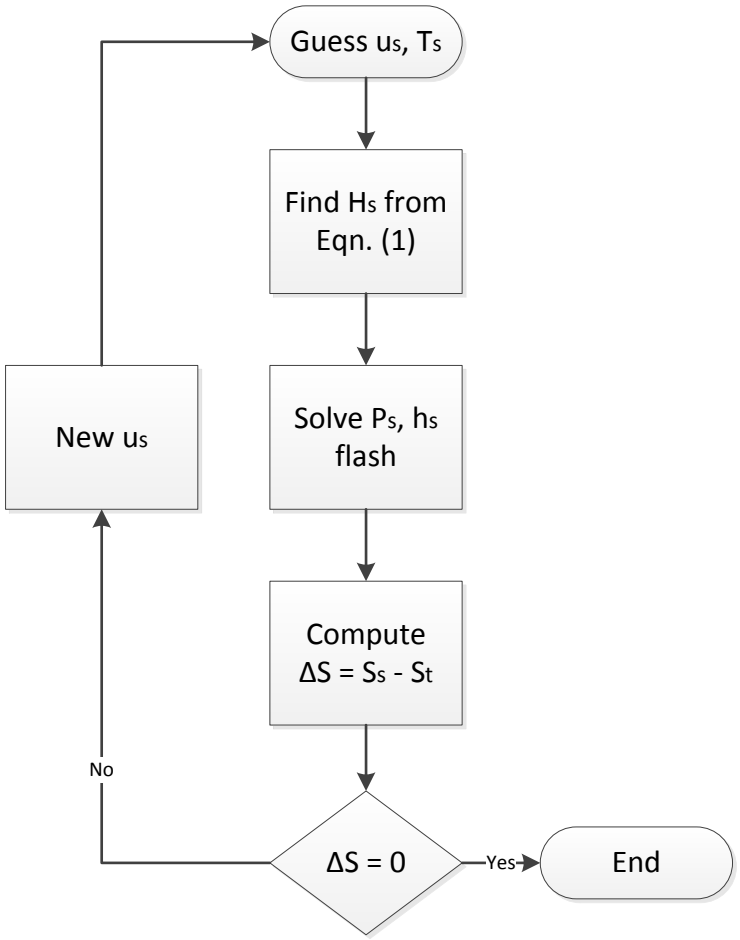

Figure 12: P-S flash flowchart

4.7.3 Procedure 2

If the flow is not subsonic in a converging nozzle, it has to be sonic, i.e., choked. The fluid velocity at the nozzle's exit plane will be equal to the sound speed at this location. As in procedure 1, it is necessary to take the energy balance and the isentropic condition into account, with an additional condition, namely that the flow is at sound speed.

Energy balance for adiabatic steady-state flow:

$$h_t = h_s\left(T_s, P_s\right) + M_s \frac{\left(c_s\left(T_s, P_s\right)\right)^2}{2} \tag{21}$$

Adiabatic reversible steady-state flow, i.e., isentropic:

$$s_t = s_s\left(T_s, P_s\right) \tag{22}$$

The numerical solution can proceed as follows:

- Guess values for T_s and P_s
- Using $\{P_s, T_s\}$, solve an isothermal flash problem (already implemented and available) and;
- Compute the corresponding sound speed (if necessary, in multiphase systems) (also available)
- Check whether the calculated values of h_t and s_t match the specification. If they don't, new estimates for T_s and P_s are necessary (generated by some numerical method) until convergence.

This solution will provide the pressure at the nozzle's exit plane. The molar flow rate will be:

$$\dot{n}_s = \frac{A_s c_s}{v_s} \tag{23}$$

The procedures described here do not require differentiating any formula to find out the critical ratio. They are general, in the sense that they are applicable to ideal gases and non-ideal fluids with single or multiple phases. Also, they should be

applicable not only to leaks from gas phases inside tanks but also to leaks from liquid phases.

4.8 Comparison with expressions for ideal gas

Most of the work published before have used the ideal gas equation of state. However, this work uses the Peng-Robinson equation of state to account for non-ideal fluid behavior. Table 3 summarizes some features of these two models.

Section 5 will show that, at low pressures, the results of Peng-Robinson model match those of the ideal gas.

Table 3: Comparison of Ideal gas EOS and P-R EOS

Ideal Gas EOS	**Peng-Robinson EOS**
Simple, analytical expression	Complicated expressions
Inaccurate to high pressure systems	• Applicable to high pressure systems • Accounts for liquid and vapor phase changes

4.9 Numerical difficulties

Throughout the thesis work, several numerical difficulties were faced while carrying out simulations. Most of the problems were due to lack of convergence, large number of iterations and bad initial estimates. These would result in problems with the UVN flash, H-S flash, convergence of fluid velocity, phase appearance or disappearance

etc. However, as these difficulties were addressed, the code improved and most, but not all, difficulties were solved.

4.9.1 Lack of convergence

- The H-S flash has several nested iterative loops. The convergence criteria has to be very tight in the innermost loops to prevent numerical instabilities in the outer loops and in the numerical integrator of the differential equations. It has not been possible to find a general set of convergence criteria that would enable the numerical convergence of all problems.
- In similar fashion, the criteria for phase stability calculations, which dictate phase addition and removal, and for flash calculations across problems with different specifications need to have compatible numerical convergence criteria. It is not possible to guarantee that the set of values currently used will work for all cases.
- When the difference between the tank and the atmospheric pressures is large, the temperature may drop in the H-S flash to levels that cause numerical difficulties to the Peng-Robinson equation of state and, ultimately lack of numerical convergence. However, it has been observed that the calculated fluid velocity converged under less severe specifications would be greater than sonic speed. Thus, this lack of convergence is interpreted as indication of sonic flow. Hence, the

procedure then jumps to sonic flow calculations, converges and moves on.

4.9.2 Iterations and initial estimates

- Because of the large number of types of iterative calculations, there are many instances where initial estimates and numerical tolerances are required. There is a complex interplay of the numerical tolerances – if one sets them loose in one part, this may prevent the convergence of another part.
- In some rare cases, the single loop numerical approach to the UVN flash would not work unless the initial estimated was extremely close to the solution. In real cases, there is no way of always getting such ultra-high quality estimates. So, as discussed, the UVN flash has a backup approach that is slower but more stable and uses multiple loops. The backup procedure was activated when necessary and promoted convergence of the UVN computations.

5. RESULTS AND DISCUSSION

This section presents examples of application of the procedure developed in this thesis. They range from simple cases with a single component and a single phase to cases with multiple phases and several components, and transition from sonic to subsonic flow at the rupture point.

5.1 Preliminary testing

The goal of the preliminary tests was to compare the results of simulator to those of two ad-hoc computations for simple situations. The first of these ad-hoc computations was done assuming the leaking fluid behaves as ideal gas. The second of them used the Peng-Robinson EOS as implemented in the XEOS package (Castier, 2008) for excel. These ad-hoc calculations can only handle single phase cases and deviations are expected to be larger for high-pressure systems because of deviations from ideal gas behavior.

The first test is for a nitrogen leak from a 2.0 L (0.002 m^3) spherical vessel at 400K and 130 bar. A circular hole with 1/8 in (0.003175 m) diameter was specified.

In this case, there is no condensation of the fluid either inside the vessel or at its exit point. The initial leak was found to be sonic. Table 4 presents the initial leak flow rates and sound speeds evaluated in each case. There is excellent agreement between the simulator and Excel results of the Peng-Robinson equation of state. These two results agree, to a lesser extent, with the ideal gas results. The discrepancy is attributed to deviations from ideal gas behavior at the initial vessel pressure of 130 bar. These

comparisons were limited to the initial flow conditions because the ad-hoc computations were not developed as dynamic simulators.

Table 4: Initial leak flow rate and sound speed: high pressure

	Peng-Robinson (Simulator)	**Peng-Robinson (Excel)**	**Ideal gas**
Flow rate (mol/s)	7.857	7.857	7.754
Sound speed (m/s)	383.44	383.73	372.07

Using the simulator, the dynamics of the vessel discharge was determined. Figures 13-15 display the results for pressure, temperature, and number of moles in the vessel as function of time. It can be seen that the simulation ran for about 6 seconds, until the pressure dropped to atmospheric pressure. There is a gradual and smooth decline in the properties traced in these figures, as expected.

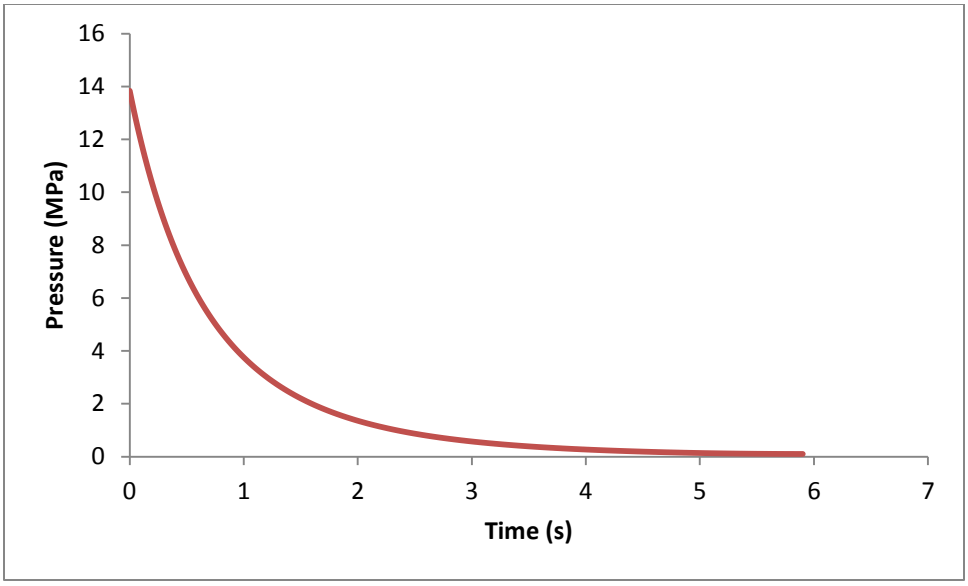

Figure 13: N_2 leak from a 0.002 m^3 vessel initially at 400K through a 1/8 in hole: pressure evolution

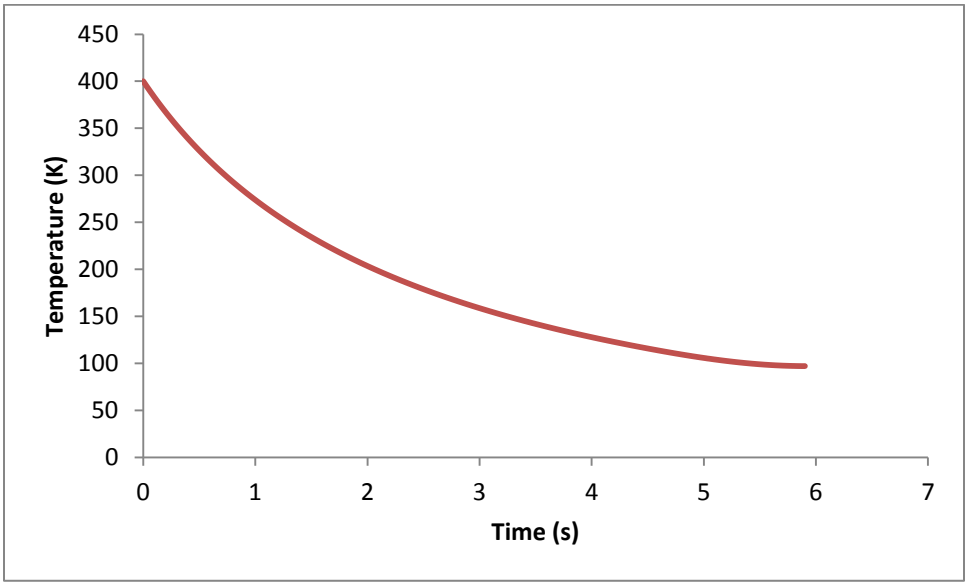

Figure 14: N_2 leak from a 0.002 m^3 vessel initially at 400K through a 1/8 in hole: temperature evolution

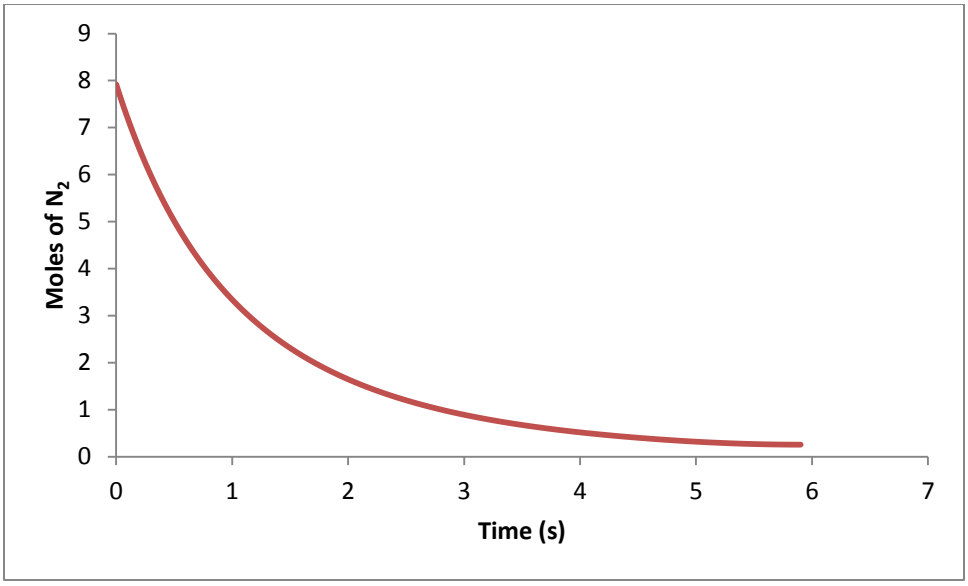

Figure 15: N_2 leak from a 0.002 m^3 vessel initially at 400K through a 1/8 in hole: mole evolution

A simulator test was conducted for nitrogen in the same vessel and initial temperature, but lower initial pressure. Table 5 shows the initial flow rate and sound speed. Compared to the previous case, in which the initial pressure was 130 bar, the initial pressure is much lower (10 bar) and there is good agreement between the ideal gas case and the two implementations of the Peng-Robinson EOS.

Table 5: Initial leak flow rate and sound speed: low pressure

	Peng-Robinson (simulator)	**Peng-Robinson (Excel)**	**Ideal gas**
Flow rate (mol/s)	0.5423	0.5423	0.5421
Sound speed (m/s)	372.38	372.58	372.07

The general observations of these initial tests are:

1. The simulator results are in good agreement with those of an independent implementation of the Peng-Robinson EOS;
2. The results are in agreement with the ideal gas EOS, especially at low pressure, as expected;
3. The dynamics of a leaking vessel containing pure nitrogen showed a smooth decay of pressure, temperature and amount in the vessel, as would be expected in such a leak.

5.2 Testing key features of the code

To test the key features of the code, a series of cases with a n-hexane + n-octane (C_6-C_8) mixture was executed. The inputs common to all simulations are shown in Table 6.

Table 6: Common inputs for simulations

Tank specifications	Cylindrical tank (Height=1m, Diameter=1m)
Volume of tank	0.7894 m^3
Initial number of moles	100
Height of rupture	0.5 m
Hole diameter	0.01 m
Initial composition	C_6: 100 moles C_8: 100 moles

The initial temperature of the fluid in the vessel was varied from 450K – 470K.

Table 7: Phase disappearance and sonic-subsonic transition for $C_6 – C_8$mixture

T(K)	No. of phases(time interval in seconds)	Sonic/Sub-sonic transition
450	2 (0-231.55)	sonic (0-154.77)
		sub-sonic (154.77-231.55)
455	2 (0-230)	sonic (0-158.64)
		sub-sonic (158.64-230)
460	2 (0-100.95)	sonic (0-156.97)
	1 (111-221)	sub-sonic (156.97-221)
465	2 (0-25)	sonic (0-153.35)
	1 (34-216)	sub-sonic (153.35-216)
467	2 (0-5)	sonic (0-152.73)
	1 (12-215)	sub-sonic (152.73-215)
468	1 (0-215)	sonic (0-152)
		sub-sonic (152-215)
470	1 (0-215)	sonic(0-152.19)
		sub-sonic(152.19-215)

Table 7 summarizes the results of these simulations. The first column is the initial temperature of the fluid in the vessel in each case. The second column reports the number of phases and time interval; for example, for an initial temperature of 465 K, the simulator predicted the existence of two phases in the vessel until 25 s. Between 25 s and 34 s, one of the phases disappears but the simulator does not compute the exact time when it happens. Between 34 s and the end of the simulation, only one phase is predicted to exist. The third column in Table 7 reports the flow regime at the rupture point. For the same initial temperature of 465K, the flow is sonic i.e, choked until 153.35 s and sub-sonic afterwards. Similar test was performed with a n-butane + n-hexane (C_4 – C_6) mixture. The TVN and leak specifications remained the same, but temperature was varied from 300K-400K. Results are shown in Table 8.

The general pattern of the results is similar to the C_6 – C_8 case. These simulations illustrate that the code is suitable for multicomponent, multiphase systems, and predicts changes in flow regime (choked to non-choked).

Table 9 illustrates cases, in which the vessel is initially loaded with 20 moles of mixture. The leak flow is sub-sonic at all times, in these cases.

Table 8: Phase disappearance and sonic-subsonic transition for $C_4 – C_6$mixture

T(K)	No. of phases(time interval in seconds)	Sonic/Sub-sonic transition
370	2 (0-176)	sonic(0-102.45)
		sub-sonic(102.45-176)
389	2 (0-174.09)	sonic (0-121.39)
		sub-sonic (121.39-174.09)
390	2 (0-90)	sonic (0-121.95)
	1 (103-182.02)	sub-sonic (121.95-182.02)
391	2 (0-50)	sonic (0-120.7)
	1 (60-180)	sub-sonic (120.7-180)
392	2 (0-25)	sonic (0-120.67)
	1 (34-178)	subsonic(120.67-178)
393	2 (0-5)	sonic(0-121.10)
	1 (14-177.7)	subsonic(121.10-177.7)
394	1 (0-177.8)	sonic(0-121.3)
		sub-sonic(121.3-177.7)
395	1 (0-179.16)	sonic (0-120.87)
		sub-sonic(120.87-179.16)
400	1 (0-177.86)	sonic (0-121.34)
		sub-sonic(121.34-177.86)

Table 9: Phase disappearance during subsonic flow

T(K)	No. of phases(time interval in seconds)	Sonic/Sub-sonic transition
394	2	Subsonic
395	2(0-30)	Subsonic
	1(44-61)	Subsonic
396	2(0-5)	Subsonic
	1(18-61)	Subsonic
397	1	Subsonic

5.3 Sensitivity analysis

The next step was to carry out a sensitivity analysis, where T,V,N and hole diameter values were varied. The results of the analysis were studied by plotting emptying time of the vessel and initial leak rate as a function of these changes, as these are the key parameters that determine the consequence of an accidental leak. These tests were conducted for Nitrogen and methane. This helped to compare the behavior of single component and multicomponent systems, by considering:

- Different temperatures: 400 K, 450 K and 500 K
- Different hole diameters: 1/4in (0.00635m) and 1/8in (0.003175m)
- Different volume: 0.003 m^3, 0.015 m^3 and 0.075 m^3
- Different number of moles: 2, 4, 6 and 8

The composition for each simulation was 99% N_2/CH_4 – 1% O_2. Before these tests, nitrogen and methane were simulated under same conditions and compared.

5.3.1 Nitrogen vs. Methane

Table 10 shows the inputs used for these simulations and the results obtained are shown in Figures 16-18.

Table 10: Inputs for N_2 and CH_4 simulations

Vessel specifications	Spherical cylinder
Volume of tank	0.0025 m^3
Initial temperature	400 K
Initial number of moles	8
Height of rupture	0.1 m
Hole diameter	0.003175 m
Initial composition	N_2/CH_4 – 99% O_2 – 1%

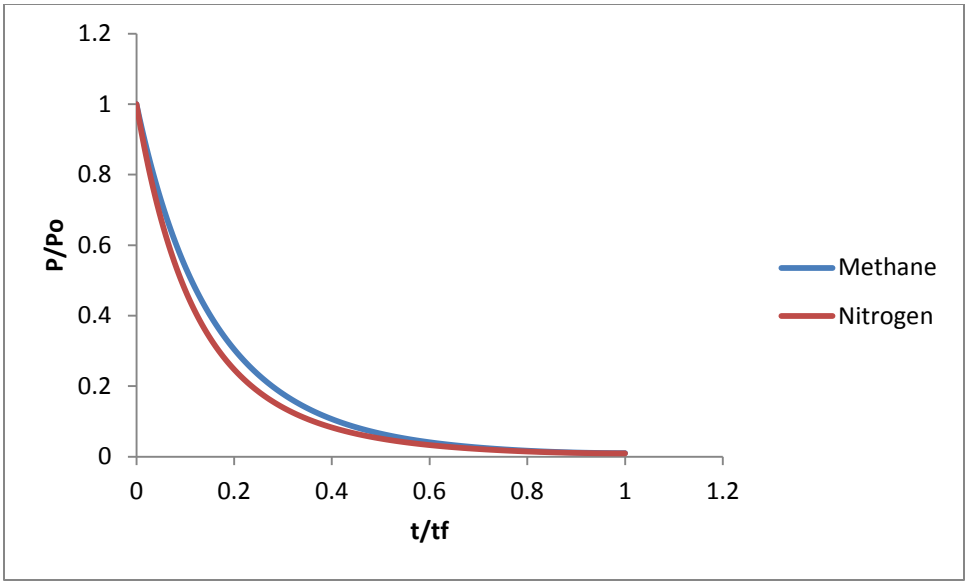

Figure 16: N_2 and CH_4 leak from a 0.0025 m^3 vessel initially at 400K through a 1/8 in hole: pressure vs. time in reduced coordinates

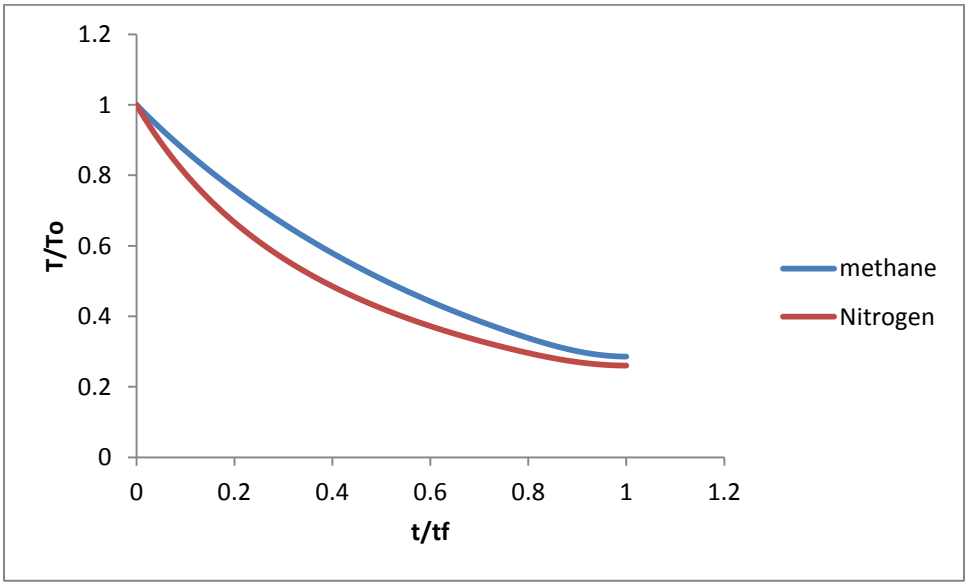

Figure 17: N_2 and CH_4 leak from a 0.0025 m^3 vessel initially at 400K through a 1/8 in hole: temperature vs. time in reduced coordinates

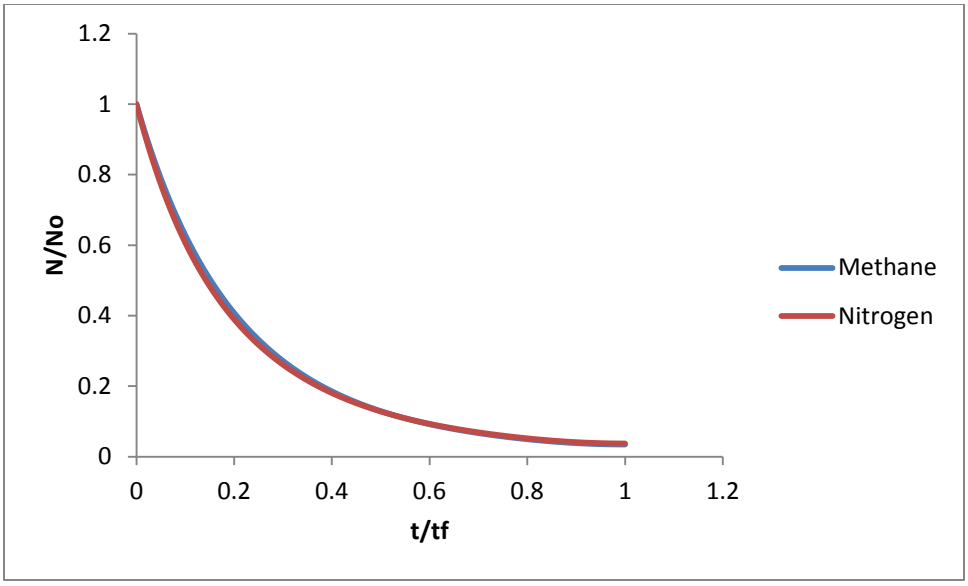

Figure 18: N_2 and CH_4 leak from a 0.0025 m^3 vessel initially at 400K through a 1/8 in hole: moles vs. time in reduced coordinates

The above graphs show that the results of nitrogen and methane are close to each other, except that the curves of methane are slightly above those of nitrogen. This was observed in the pressure and temperature graphs. In the mole vs. time graphs, both the curves overlap each other. The slight deviation could be due to higher heat capacity (C_v) value of methane. Because of a higher C_v value, there will be less temperature decrease in case of methane. Hence, the curve of methane is slightly above that of nitrogen. Otherwise, the results are good and as expected. The pressure curve has come out smooth and perfect, touching the ratio of 1 at both the axes.

5.3.2 Effects of varying T,V,N and hole diameter

The next test was to see how initial flow rate and emptying time changes by varying hole diameter, temperature, volume and number of moles, as mentioned before.

These changes were plotted for both nitrogen and methane simulations, and were compared. The graphs can be seen in Figure 19-26. All of the graphs show expected trends.

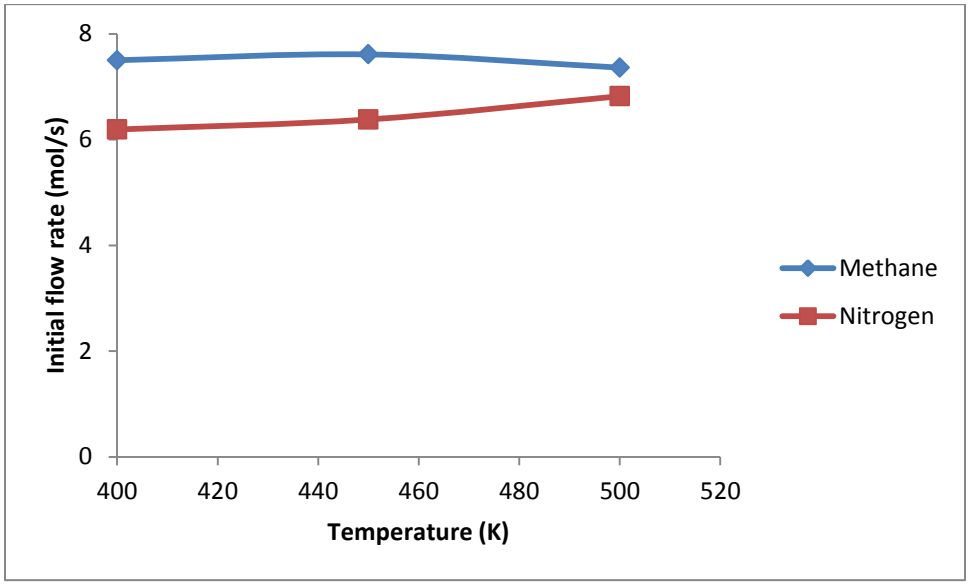

Figure 19: N_2 and CH_4 leak from a 0.0025 m3 vessel consisting of 8 moles, through a 1/8 in hole: Initial flow rate vs. temperature

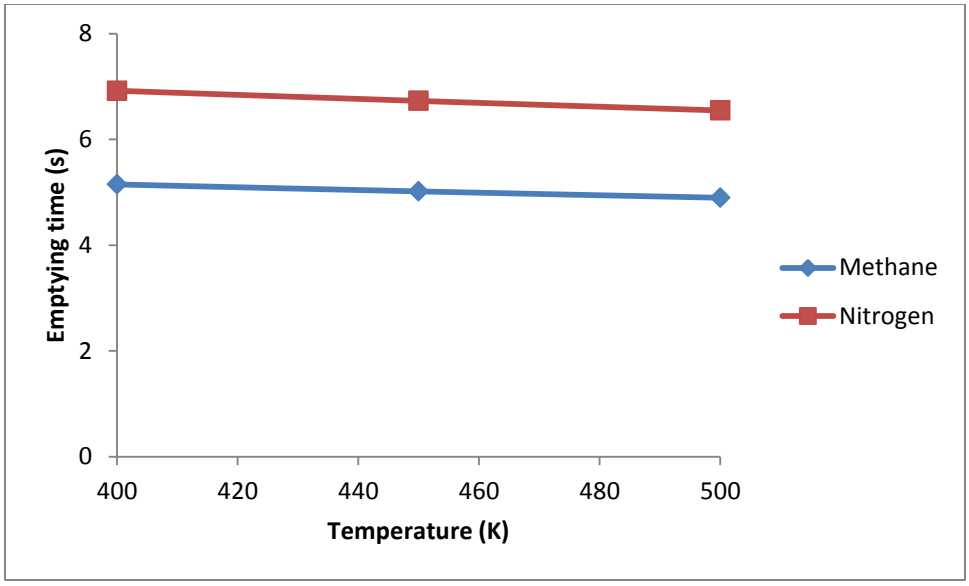

Figure 20: N_2 and CH_4 leak from a 0.0025 m3 vessel consisting of 8 moles, through a 1/8 in hole: Emptying time vs. temperature

There is a huge difference in the emptying times of nitrogen and methane simulations. Also, there is only a slight change in the emptying time with increase in temperature. On the other hand, the initial flow rate curves of nitrogen and methane see a good difference at lower temperatures, but at higher temperatures the difference is less.

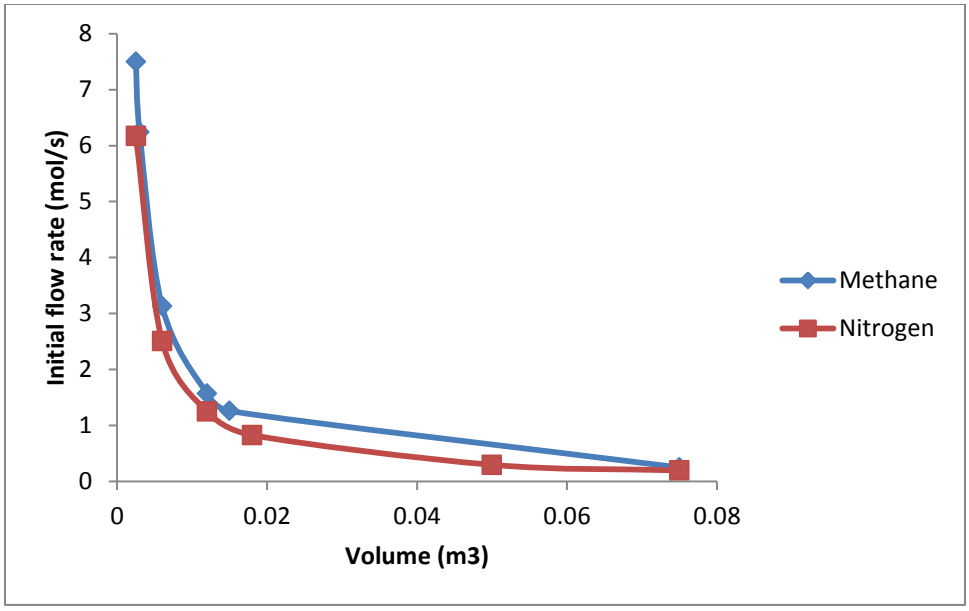

Figure 21: N_2 and CH_4 leak from a vessel at 400 K, consisting of 8 moles, through a 1/8 in hole: Initial flow rate vs. volume

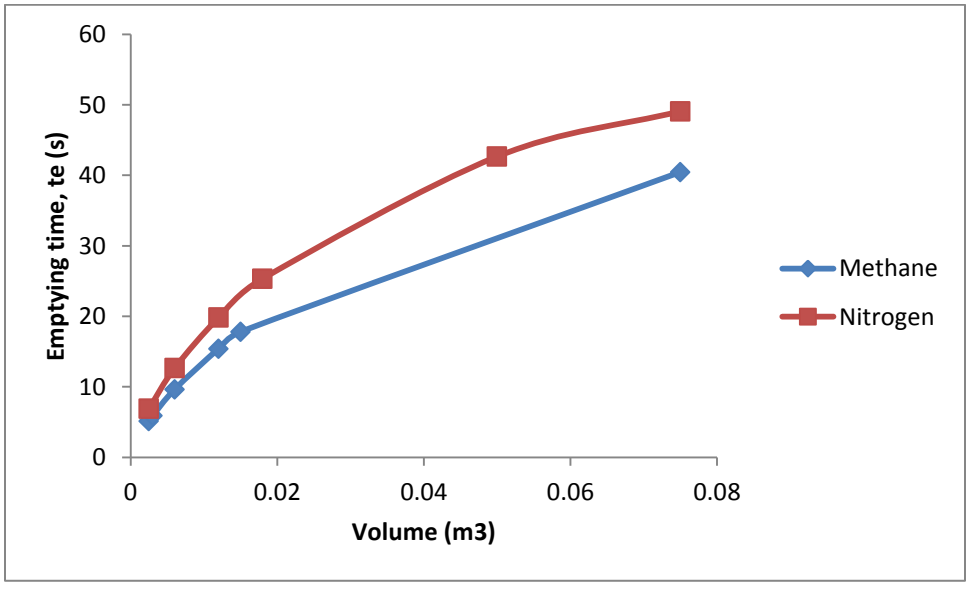

Figure 22: N_2 and CH_4 leak from a vessel at 400 K, consisting of 8 moles, through a 1/8 in hole: Emptying time vs. volume

Figure 21 and Figure 22 show expected trends. As volume increases, the vessel takes more time to empty. However, as the volume is increased for a given number of moles, the pressure within the vessel decreases and hence, the flow rate tends to decrease.

Figure 23 and Figure 24 show how the initial flow rate and emptying time vary with increasing number of moles. For a given volume as the number of moles increases, the flow rate and emptying time increase.

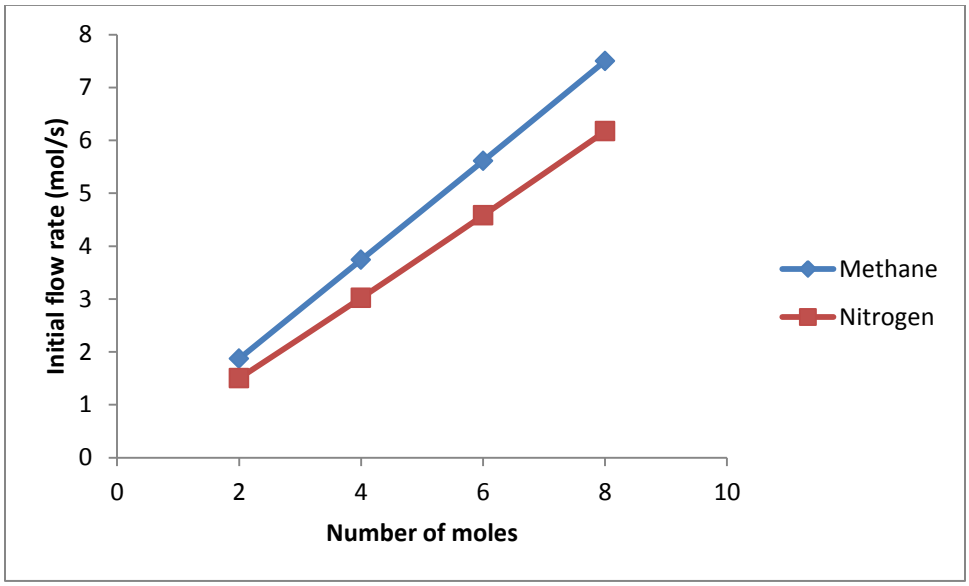

Figure 23: N_2 and CH_4 leak from a 0.0025 m^3 vessel at 400 K, consisting of 8 moles, through a 1/8 in hole: Initial flow rate vs. moles

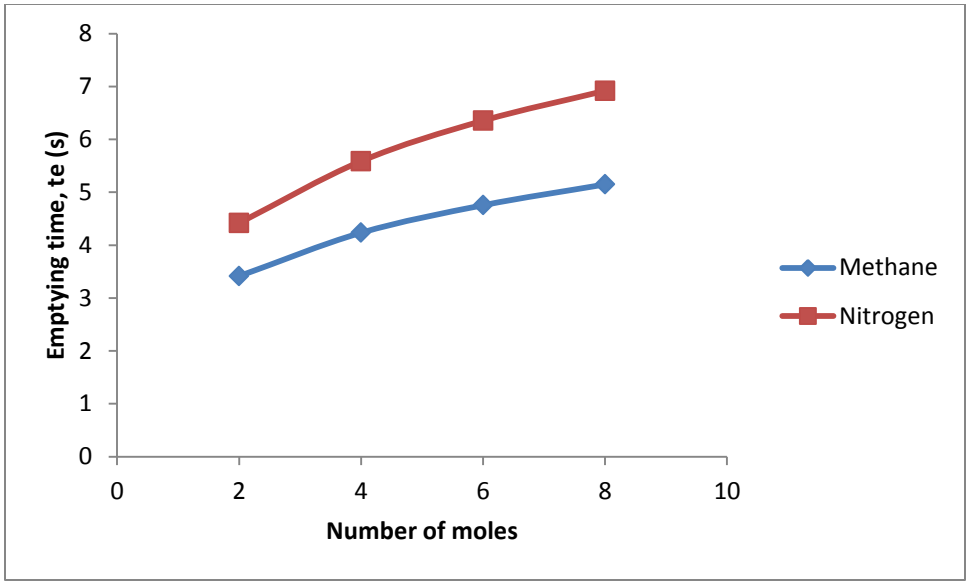

Figure 24: N_2 and CH_4 leak from a 0.0025 m^3 vessel at 400 K, consisting of 8 moles, through a 1/8 in hole: Emptying time vs. moles

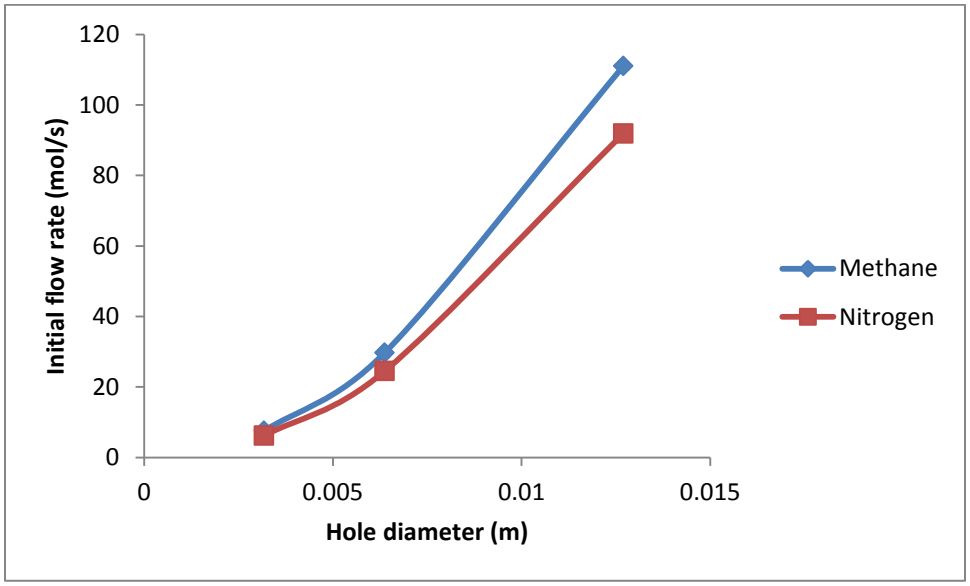

Figure 25: N_2 and CH_4 leak from a 0.0025 m^3 vessel at 400 K, consisting of 8 moles, through a 1/8 in hole: initial flow rate vs. hole diameter

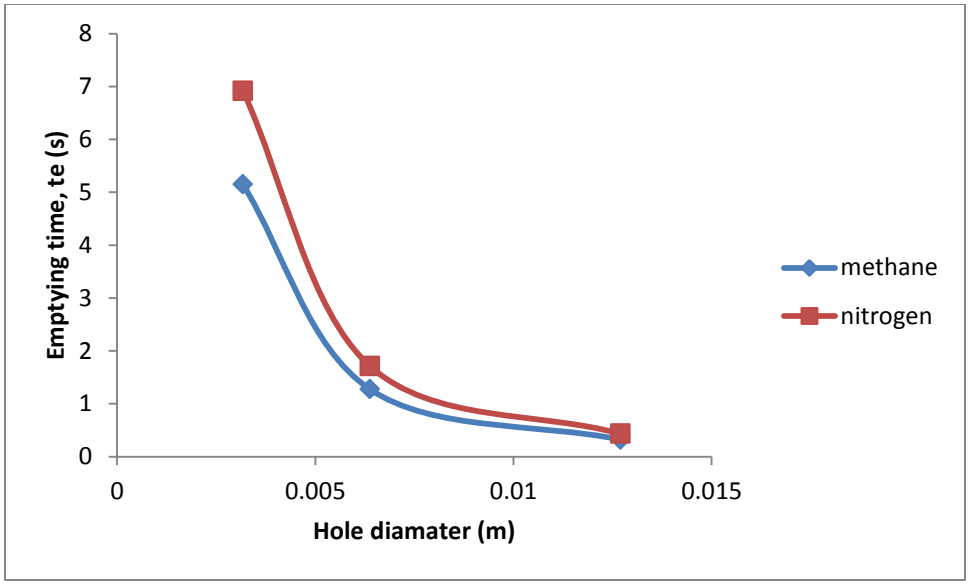

Figure 26: N_2 and CH_4 leak from a 0.0025 m^3 vessel at 400 K, consisting of 8 moles, through a 1/8 in hole: Emptying time vs. hole diameter

Figure 25 and 26 show expected trends. As the hole diameter increases, the cross sectional area for the fluid to leak increases and hence, the flow rate increases. Consequently, the emptying time would be less.

One observation common to all of the above graphs is that, the methane curve was above when initial flow rate was plotted, and was below nitrogen when emptying time was plotted.

5.4 Validation

This section shows examples taken from published papers and compares these with those from the simulator. After sensitivity analysis, it was decided to run a few examples from published papers and compare the results.

5.4.1 Raimondi (2012)- Rigorous simulation of LPG releases from accidental leaks

Raimondi (2012) simulated the Viareggio Railway station accident that took place on June 29, 2009. The accident occurred due to LPG release causing large number of fatalities. The focus of his study was on the discharge time required to empty the damaged vessel, which is considered as rigid and with perfect thermal insulation. The simulation uses cubic equations of state, Soave-Redlich-Kwong or Peng-Robinson, for vapor-liquid equilibrium, the Lee-Kesler model for enthalpy, entropy and density calculations, and ideal gas sound speed calculations. Two different scenarios were considered – bottom leak and top leak. The initial conditions used in the simulations are shown in Table 11.

Table 11: Initial conditions for simulation of LPG release (Raimondi, 2012)

Pressure	15 bar
Temperature	71.69^{o}C
Molar composition of components	Ethane: 2.25% Propane: 32.7% n-butane: 64.21% n-pentane: 0.84%
Mass	45000 kg
Leak area	0.01 m^2
Discharge coefficient	0.6

Figure 27 reproduces Raimondi's results for a leak from the bottom of the tank. There is a change of slope at about 15 min (900 seconds) in his results. According to Raimondi (2012), at this time, the liquid is all drained out and there is only vapor inside the tank, causing the abrupt property changes.

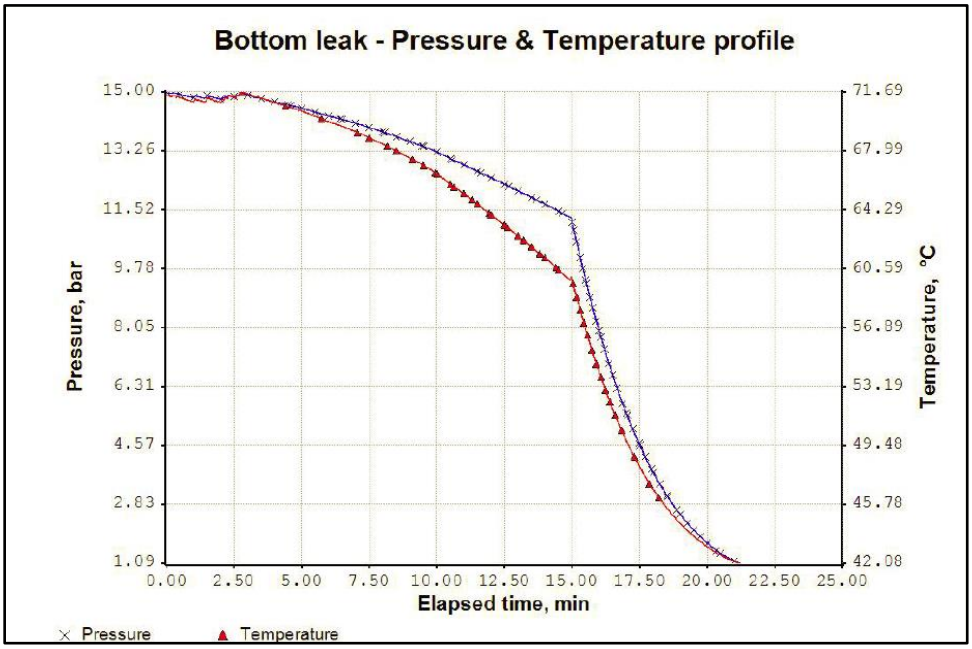

Figure 27: Bottom leak results as shown in the paper (Raimondi, 2012)

This bottom leak was simulated in this thesis, from equivalent initial conditions. In the simulator developed here, the initial fluid temperature and the molar amounts of each component are specifications. Also, the shape and size of the vessel and of the hole on its wall need to be specified, and not only their respective volume and area. Table 12 summarizes these specifications, which are such that the initial mass in the vessel is

45000 kg and its molar composition matches the values shown in Table 11. With the temperature and vessel volume shown in Table 12, the initial pressure is 15 bar, also as in Table 11. The hole position is as low as possible in the vessel and its diameter is such that the hole area is equal to 0.1 m^2, which was the value used by Raimondi (2012).

Table 12: Initial conditions for simulation of LPG release (this thesis)

Vessel type	horizontal cylinder
Vessel volume	115.7704539 m^3
Vessel length	15.95 m
Temperature	344.7 K
Molar amounts	Ethane: 19095.56 Propane: 277522.11 n-butane: 544944.80 n-pentane: 7129.01
Hole type	circular
Hole diameter	0.11283792 m
Hole position	0.05641896 m from the vessel's bottom

Unlike Raimondi's simulation, which uses several methods to compute the thermodynamic properties, all of them consistently come from the same model (the Peng-Robinson EOS) in this work. However, the method used here does not include the

discharge coefficient. Given the similarities and differences in modeling, the expectation is to obtain comparable but not identical results.

Figure 28 and Figure 29 display the temperature and pressure profiles predicted by the computational procedure developed in this thesis. There are several features to note. One of them is that the simulation stops at 736.9 s when the pressure of the fluid in the vessel is predicted to be equal to 0.10133 MPa, which is practically equal to the atmospheric pressure (0.10132 MPa). Raimondi's simulated time is longer and ends at about 1270 s. Since the discharge coefficient is the ratio of the actual discharge to the theoretical discharge, Raimondi's discharge under theoretical conditions can be roughly estimated as his calculated discharge time (1270 s) multiplied by the discharge coefficient (0.6), i.e., 762 s. The result of this thesis, 736.9 s, is about 3.3% smaller than this value. An important difference is the final temperature, which only drops to about 315.2 K (Figure 27) at the end of Raimondi's (2012) simulation, while it reaches 257.0 K in this thesis. As per private communications with this author, there seems to be a difference in the way the dynamic energy balance equation is formulated. The formulation used in this thesis follows the general energy balance equation for open dynamic systems commonly discussed in thermodynamic textbooks and widely used for engineering calculations and design.

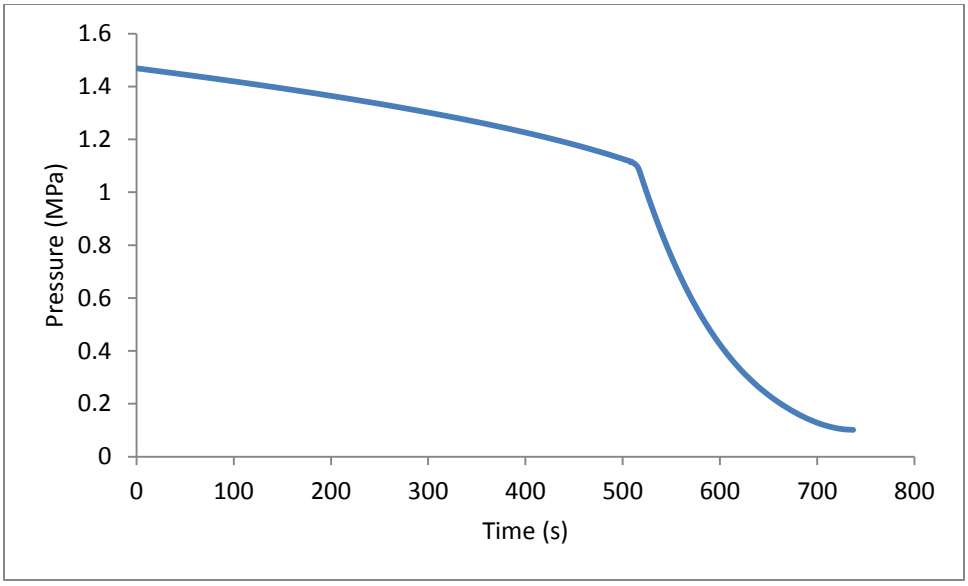

Figure 28: Predicted pressure of the fluid in the vessel during bottom leak

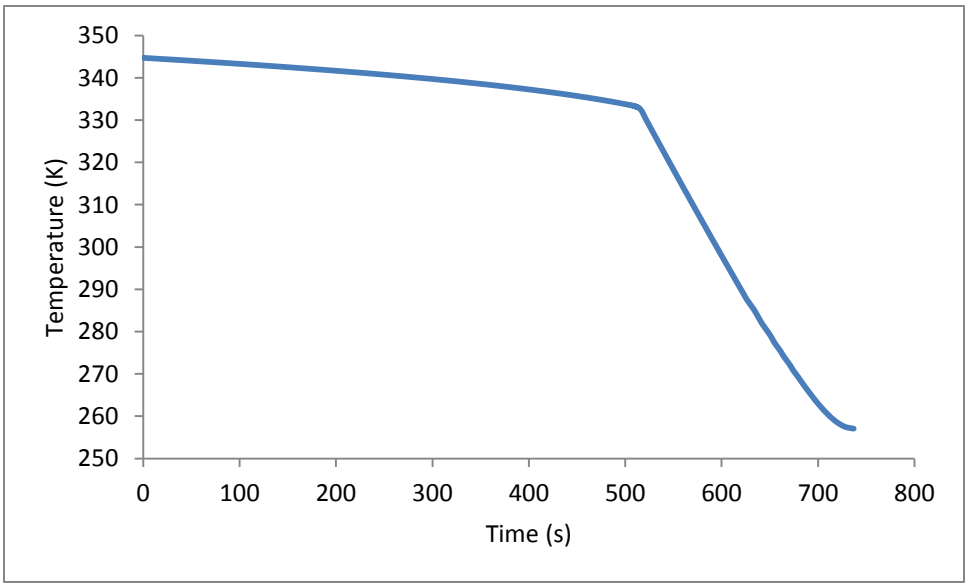

Figure 29: Predicted temperature of the fluid in the vessel during bottom leak

The temperature and pressure profiles exhibit a change of slope that occurs when the liquid phase in the vessel disappears at about 519.3 s, i.e., at about 70.5% of the total discharge time (736.9 s). In Raimondi's example, the liquid phase disappears at about 896 s and, likewise, this corresponds to 70.5% of the total discharge time (1270 s) of his simulation. When the liquid phase disappears, the results of this thesis indicate that the temperature and pressure of the fluid in the vessel are equal to 331.2 K and 1.06 MPa, respectively. The corresponding values according to Raimondi's simulation are 332.2 K and 1.14 MPa. The relative deviations in temperature and pressure are equal to 0.3% and 7.0%, respectively.

The leak flow is choked (sonic) from the beginning of the simulated time until about 674 s, when it becomes non-choked (subsonic). It is predicted to have two phases throughout the simulated time.

Figure 30 shows the component molar leak flow rates. The flow rates of all components exhibit small changes as long as there is liquid in the vessel. When the liquid disappears at about 519.3 s, a sharp decrease is predicted for all components, except ethane, which is the most volatile component of the mixture. After a short peak, the leak flow rate of ethane also decreases. It is also interesting to observe the fluctuations in the flow rate curves toward the end of the simulated time, most noticeably for n-pentane. These are numerical fluctuations unrelated to the underlying physical phenomena.

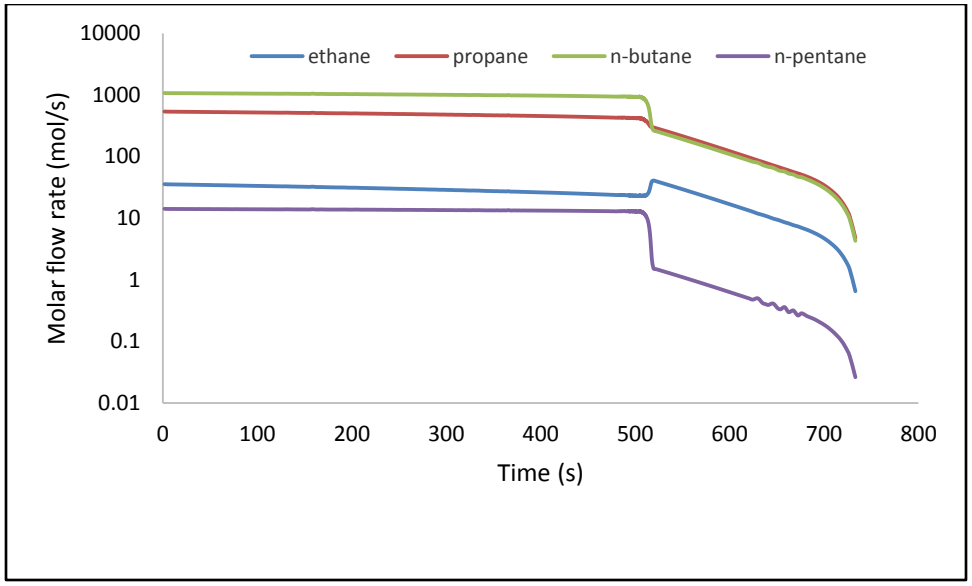

Figure 30: Predicted exit component molar flow rates during bottom leak

A detailed model, such as that used here, provides a wealth of information about the fluid inside the vessel and the fluid that leaks from it. Figure 31 displays the amount of each component inside the vessel as function of time. It is interesting to compare the ratio between the final and initial amounts of each component, which are equal to 2.04%, 1.01%, 0.450%, and 0.182%, for ethane, propane, n-butane, and n-pentane, respectively. As expected, the ethane has the largest ratio and n-pentane, the smallest.

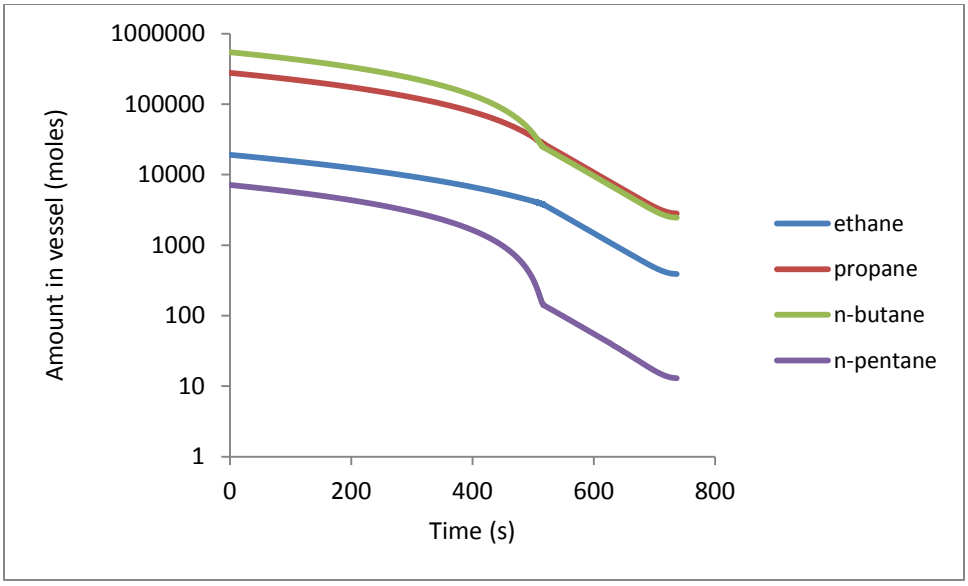

Figure 31: Predicted component amounts in the vessel during bottom leak

Figure 32 shows the volume occupied by the liquid phase until its disappearance at about 519.3 s. In the final seconds before the complete depletion of the liquid phase, when its volume is less than 1.39 m^3, the leaking orifice is only partially covered by liquid. This is taken into account in the calculations by weighting the contributions of the liquid and vapor phases inside the tank according to the area of the hole they cover.

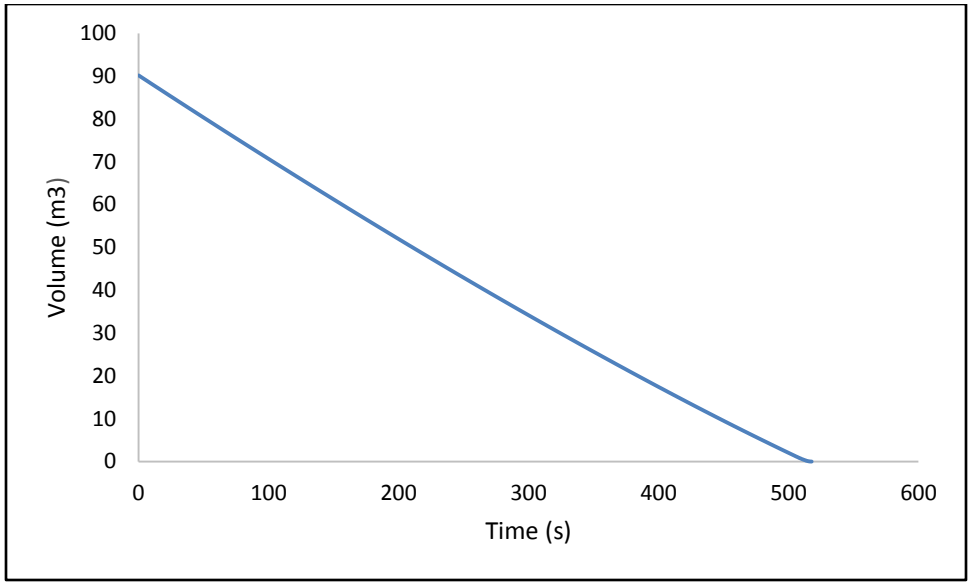

Figure 32: Predicted volume of the liquid phase in the vessel during bottom leak

Figure 33 and 34 show the predicted mass density of the vapor and liquid phases, respectively. They follow opposite trends. The vapor phase density decreases and more sharply after the disappearance of the liquid phase, as expected. The liquid phase density increases, as consequence of the temperature drop, but the relative change in is smaller than for the vapor, which is also expected because the liquid phase is much less compressible than the vapor phase.

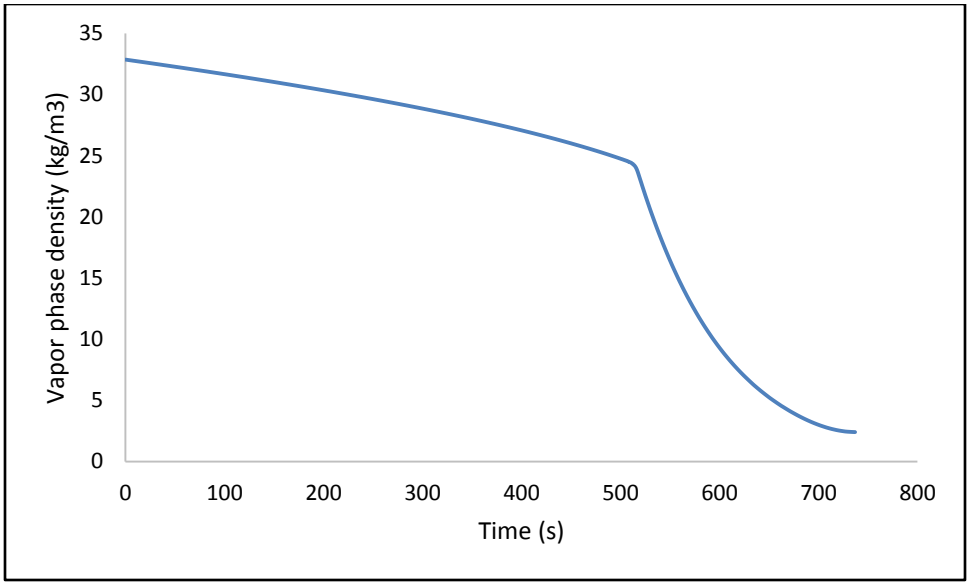

Figure 33: Predicted vapor phase density in the vessel during bottom leak

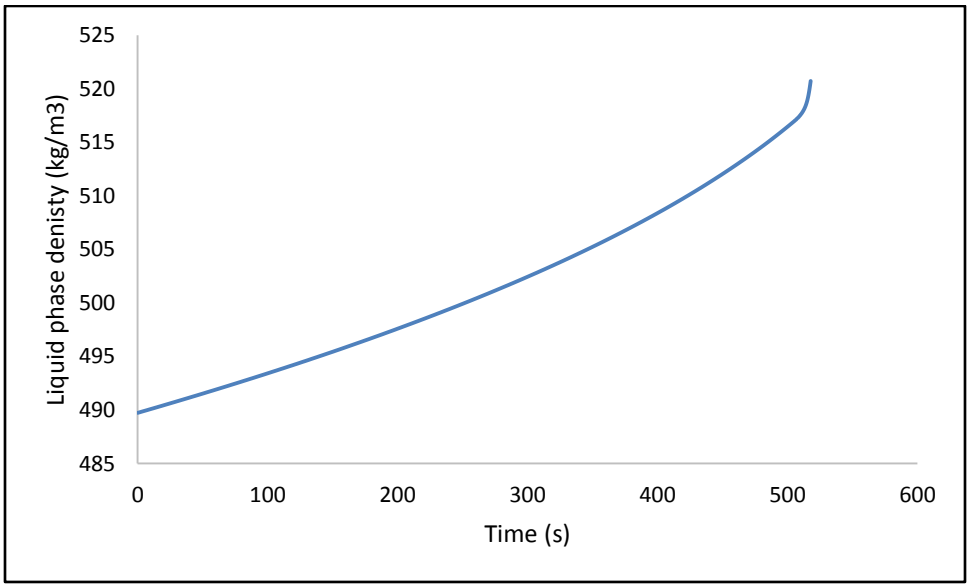

Figure 34: Predicted liquid phase density in the vessel during bottom leak

The overall analysis of this example shows generally good agreement with the results reported by Raimondi (2012), especially if one rescales time based on the coefficient of discharge. The liquid phase in the tank is predicted to disappear at 70.5% of the total discharge vessel time, both in this thesis and in Raimondi's (2012) work. The predicted temperature and pressure at the moment the liquid phase disappears agree within 0.3% and 7.0%, respectively. Raimondi's (2012) work does not report the profiles for other properties and, thus, no direct comparison is possible. However, it should be stressed that the predicted values of all of them exhibit meaningful trends.

5.4.2 Norris and Puls (1993)

Norris and Puls (1993) published two papers that discussed the new models they had developed for single phase and multiphase blowdown, and hydrocarbon blowdown from vessels and pipelines. These papers also published results of simulations carried out to test their models and compared them with experimental results. Out of these, one simulation was repeated for validation of this thesis work. Details of the simulation are shown in Table 13.

Figure 35 reproduces the results for leak flow rate of the original publication, which are at the top left part of the plot for a hole diameter of 0.402 in. Figure 36 displays the results of this thesis for the same initial conditions, with the time axis extended to 50 s to facilitate visual comparison with Figure 35. According to the results of this thesis, the initial flow rate is equal to about 5.6 lbm/s, which is in good agreement with the simulated result of Figure 35 (denote as the "FRICUP" curve). Both differ from the experimental result, which is slightly larger than 3 lbm/s. The last simulated point in

Figure 35 is at about 8 s with a flow rate of 0.5 lbm/s, while the corresponding value in this work is equal to 0.47 lbm/s, and the experimental value is about 0.7 lbm/s. These comparisons indicate that, for this case, the models of Norris and Puls (1993) and of this thesis agree very well with each other and both predict the trend of the experimental data, despite quantitative deviations.

Table 13: Inputs for blowdown simulation of air

Vessel type	Horizontal cylinder
Vessel height	1.524 m
Vessel volume	0.0504 m^3
Pressure	138 bar
Initial temperature	300K
Molar amounts	Nitrogen: 223.08 Oxygen: 55.77
Hole type	Circular
Hole diameter	0.402 in (0.00102108 m)
Hole position	0.2 m from bottom of the vessel

It should be remarked that the simulation of this thesis stopped at 9.75 s, when the pressure of the fluid in the vessel was equal to 0.44 MPa. From the beginning of the simulation, the exit flow is predicted to be choked and contain a single gas phase. During

the leak, the temperature and pressure inside the vessel drop, as shown in Figure 37 and 38, and they are even lower at the exit plane. At about 10 s, the simulation predicts that the onset of air condensation at the exit plane, i.e., a condition close to the dew point of dry air. This condition is determined by solving the flash at the exit point, which has specifications of enthalpy and entropy and uses nested loops in temperature and pressure to find the state of the fluid. Thus, it has multiple embedded convergence criteria for the equilibrium calculations and for phase stability analysis. Numerical fluctuations and lack of accuracy in these calculations propagated to the numerical integrator of the ordinary differential equations of the model, preventing its progress. Despite several attempts, it was not possible to find a set of values of these numerical criteria that allowed the simulation to proceed until the pressure within the vessel reached the atmospheric pressure. Possible ways of fixing this problem are the use of a flash procedure without nested loops and of another numerical integrator of ordinary differential equations. It is also interesting to observe that the simulated curve in Figure 35 stops at 8 s. Given that the predicted discharge rates in the two simulations are similar and that the pressure in the vessel is still equal to 0.44 MPa at 9.75 s, it is unclear whether the final pressure in the Norris and Puls (1993) simulation is the atmospheric pressure.

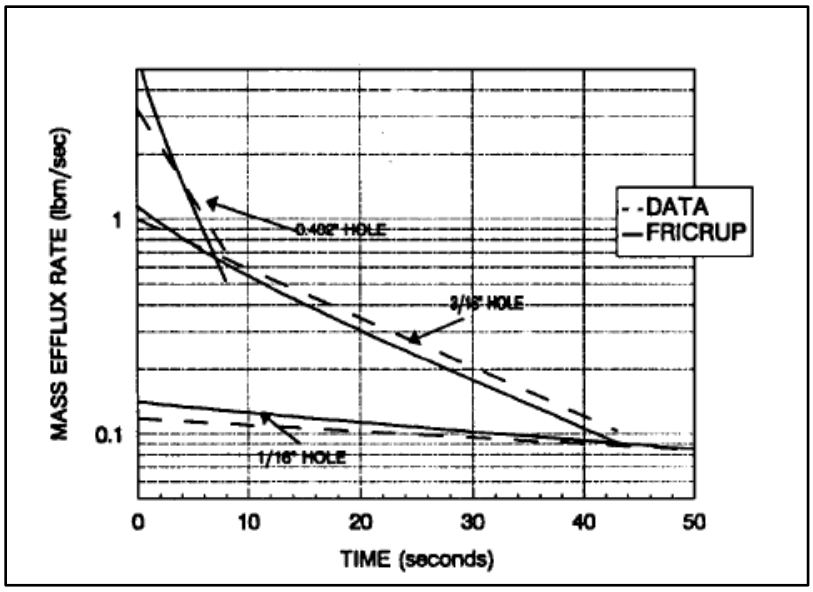

Figure 35: Flow rate vs. time for blowdown of air as shown in the paper (Norris & Puls, 1993)

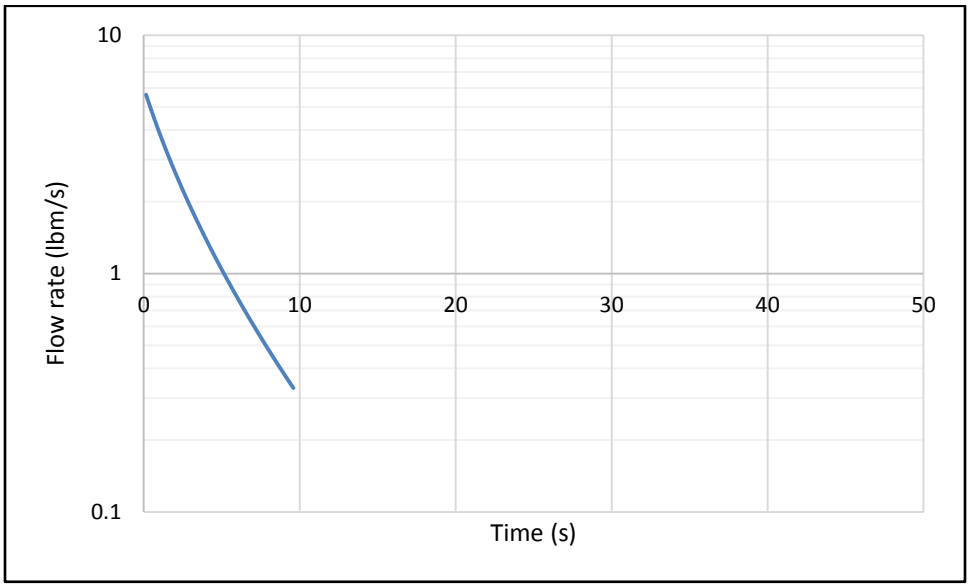

Figure 36: Flow rate vs. time for blowdown of air

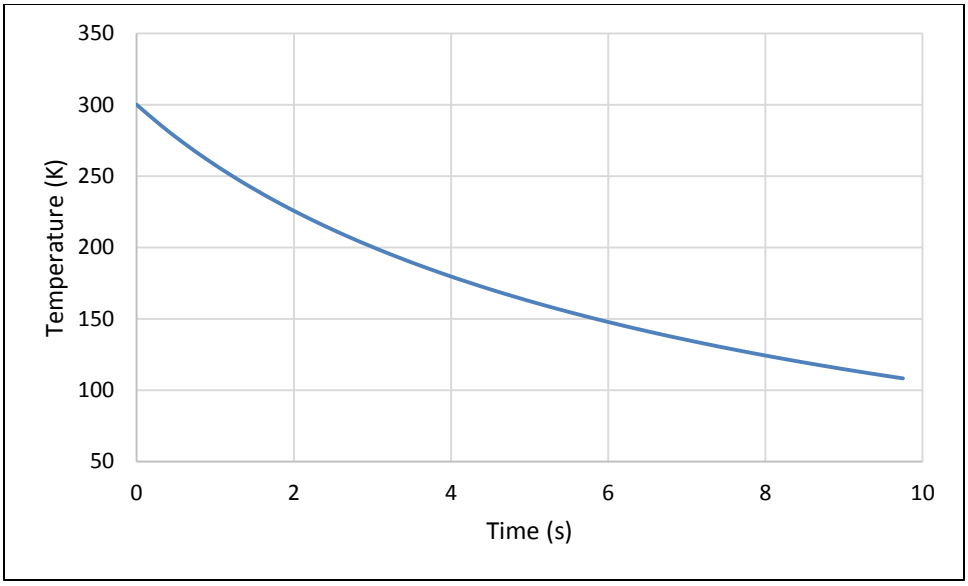

Figure 37: Temperature of fluid in the vessel vs. time for blowdown of air

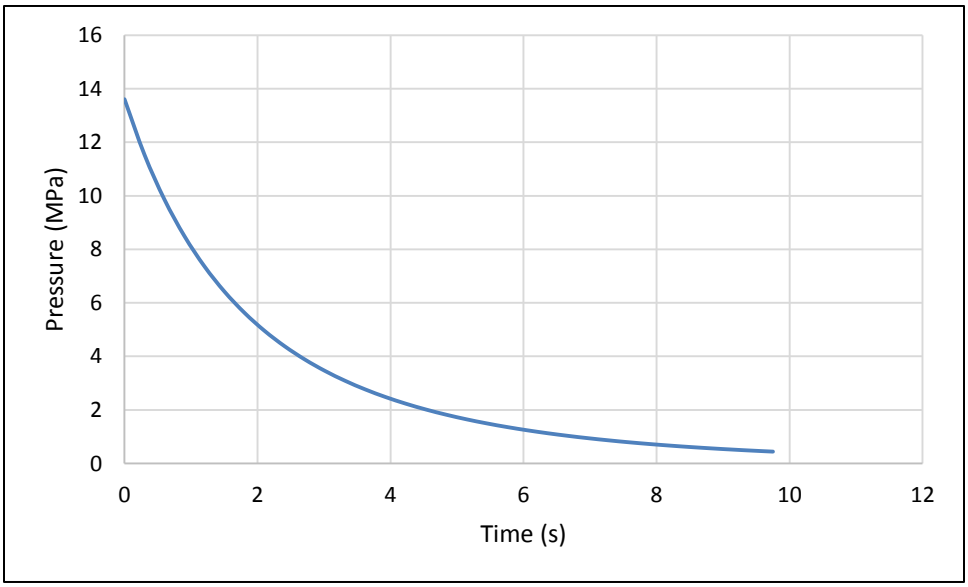

Figure 38: Pressure of fluid in the vessel vs. time for blowdown of air

6. CONCLUSION

The state of fluids inside leaking rigid pressurized vessels and the conditions of the leak streams from pressurized vessels were found by solving a system of differential algebraic equations. In it, the dynamic mass and energy balances for the vessel are the differential equations, whose stepwise numerical solution provides the values of the internal energy and molar amounts of each component of the fluid. These differential equations are coupled to several algebraic problems in the simulator. One of them is the problem of finding the state of the fluid in the vessel by maximizing its entropy. This is equivalent to assuming that there is instantaneous phase equilibrium in the vessel. A second algebraic problem is to find the fluid properties at the leaking point, which are different from those of fluid inside the vessel. This is done under the assumption that the leaking point is the throat of an adiabatic, converging nozzle whose operation is isentropic. This leads to a flash problem whose specifications are the fluid's enthalpy, entropy, and molar amounts of each component. The ultimate goal of this calculation is to find the flow rate and properties of the leaking stream. However, this problem is constrained by the fact the flow is either sonic (choked) or subsonic (non-choked), but not supersonic. It should be noted that, depending on conditions, the fluid may have one or more phases as it leaves the leaking vessel. Therefore, a third algebraic problem is to compute sound speeds in multiphase systems to establish whether the leak flow is choked.

In addition to these core differential and algebraic problems, several ancillary details are relevant to account for the effect of: (a) tank geometry; (b) hole geometry; (c) leak position.

A code was developed in Fortran to integrate these calculation procedures. In any given simulation, each of them may be executed hundreds or thousands of times. Computational reliability, i.e., running faultless in all cases, is the single most important goal to be achieved. Experience accumulated during this work has shown that the program runs well for several cases, but occasionally fails to converge for some specifications, despite many efforts to achieve numerical convergence in all cases.

These occasional failures seem to originate from two sources. One of them is the issue of providing good initial estimates for the numerical convergence of all the algebraic problems that are part of the overall procedure. In all cases, information about previous time steps was used to generate initial estimates but this does not guarantee success in all situations. Another possible source of numerical difficulties is that some of the phase equilibrium algorithms use nested iterative loops, whose numerical convergence criteria need to be carefully balanced to avoid numerical instabilities. In some problems, it has not been possible to find the proper balance. Therefore, the simulator results exhibited meaningful qualitative trends and it could handle complex cases, in good agreement with literature. However, its less-than-perfect numerical performance opens the possibility of many future developments, outlined in the next section.

7. FUTURE WORK

From the simulations carried out and the results obtained, it is clear that there is a need for more tests to assess the reliability of the numerical methods used and the quality of the estimates utilized for each of them, leading to their refinement. It is recommended to replace the flash calculations that use nested loops, by procedures that use a single loop, possibly leaving a nested loop procedure as backup method, as the isochoric-isoenergetic (UVN) flash currently does. The expectation is that this will reduce numerical fluctuations that affect the flash calculations themselves and the performance of the ordinary differential equation integrator. Another possibility to alleviate the numerical difficulties is to test the performance of other ordinary differential equation integrators.

An additional issue is the overall speed of the simulations. In all cases, the simulations took longer in a typical current personal computer than the timespan they model. Thus, they would be unsuitable to assist in real time decisions in the case of an accidental fluid release. While it is reasonable to expect that faster computers will alleviate or eliminate this problem, another possibility is to take advantage of the parallel processors available in most modern personal computers or in clusters. Parallel algorithms for the integration of ordinary differential equations exist and can be tested for the application of this thesis.

The issue of computation speed is particularly important if one considers the accurate simulation of leaks from systems that contain natural gas. Another extension of

this thesis is adding the GERG-2008 equation of state to the code. This computationally demanding, highly accurate thermodynamic model will be adopted as an ISO standard for the design of natural gas processing units. Therefore, its use is particularly relevant to the State of Qatar. Another possible extension is to include the effect of liquid swelling due to disorderly vaporization during a vapor phase leak. From the user's perspective, the development of a graphical interface for the simulator should facilitate its application.

Finally, the procedure was developed and test for non-reactive systems. However, leaks may occur in reactive systems because of, for example, runaway reactions. An extension of the procedure developed here to model leaks from reactive systems will give the opportunity to quantify their effects and could be useful for the design of relief systems.

REFERENCES

Bendlk, K. H., Malnes, D., Moe, R. & Nuland, S. (1991). The dynamic two-fluid model OLGA : Theory and Application. *SPE Production Engineering*, *6*(2), 171-180. SPE 19451.

Castier, M. (2008). XSEOS: An open software for chemical engineering thermodynamics. *Chemical Engineering Education*, *42*(2), 74-81.

Castier, M. (2009). Solution of the isochoric–isoenergetic flash problem by direct entropy maximization. *Fluid Phase Equilibria*, *276*(1), 7–17.

Castier, M. (2010). Dynamic simulation of fluids in vessels via entropy maximization. *Journal of Industrial and Engineering Chemistry*, *16*(1), 122–129.

Castier, M. (2011). Thermodynamic speed of sound in multiphase systems. *Fluid Phase Equilibria*, *306*(2), 204–211.

Cumber, P. S. (2001). Predicting outflow from high pressure vessels. *Institution of Chemical Engineers*, *79*(B), 13–22.

Diener, R., & Schmidt, J. (2005). Sizing of throttling device for gas/liquid two-phase flow part 2: control valves, orifices, and nozzles. *Process Safety Progress*, *24*(1), 29–37.

Esposito, R. O., Castier, M., & Tavares, F. W. (2000). Calculations of thermodynamic equilibrium in systems subject to gravitational fields. *Chemical Engineering Science*, *55*(17), 3495–3504.

Fthenakis, V. M. (1993). Discharge rates through holes in process vessels and piping. In: Fthenakis, V.M (ed), *Prevention and Control of Accidental Releases of Hazardous Gases* (94-159). New York: John Wiley & Sons.

Giacchetta, G., Leporini, M., Marchetti, B., & Terenzi, A. (2014). Numerical study of choked two-phase flow of hydrocarbons fluids through orifices. *Journal of Loss Prevention in the Process Industries*, *27*(1), 13-20.

Goncalves, F. ., Castier, M., & Araujo, O. Q. . (2007). Dynamic simulation of flash drums using rigorous physical property calculations. *Brazilian Journal of Chemical Engineering*, *24*(02), 277–286.

Haque, A., Richardson, S., Saville, G., & Chamberlain, G. (1990). Rapid depressurization of pressure vessels. *Journal of Loss Prevention in the Process Industries*, *3*(1), 4–7.

Fisher, H.G., Forrest, H.S., Grossel, S.S., Huff, J. E., Muller, A.R, Noronha, J.A., Shaw D.A., Tilley, B.J. (1993). Pressure relief system flow: Results of the DIERS phase II projects. In: *Emergency Relief System Design Using DIERS Technology: The Design Institute for Emergency Relief Systems (DIERS) Project Manual* (51-72). New York: John Wiley & Sons.

Johnson, D. W., & Woodward, J. L. (1999). *RELEASE: A Model with Data to Predict Aerosol Rainout in Accidental Releases.* New York: Center for Chemical Process Safety, AIChE.

Lenclud, J., & Venart, J. E. S. (1996). Single and two-phase discharge from a pressurized vessel. *Rev Gen Therm*, *35*, 503–516.

Leung, J. C. (1990). Two-phase flow discharge in nozzles and pipes-a unified approach. *Journal of Loss Prevention in the Process Industries*, *3*(1), 27-32.

Mahgerefteh, H., Falope, G. B. O., & Oke, A. O. (2002). Modeling blowdown of cylindrical vessels under fire attack. *AIChE Journal*, *48*(2), 401–410.

Mahgerefteh, H., Saha, P., & Economou, I. G. (2000). Modeling fluid phase transition effects on dynamic behavior of ESDV. *AIChE Journal*, *46*(5), 997–1006.

Mahgerefteh, H., & Wong, S. M. . (1999). A numerical blowdown simulation incorporating cubic equations of state. *Computers & Chemical Engineering*, *23*(9), 1309–1317.

Michelsen, M. L. (1999). State function based flash specifications. *Fluid Phase Equilibria*, *158-160*, 617–626.

Nielsen, D. S. (1991). Validation of two-phase outflow model. *Journal of Loss Prevention in the Process Industries*, *4*(4), 236–241.

Norris, H. L., & Puls, R. C. (1993a). Single-phase or multiphase blowdown of vessels or pipelines. Presented at SPE Annual Technical Conference and Exhibition, 3-6 October, 1993, Houston, Texas.

Norris, H. L., & Puls, R. C. (1993b). Hydrocarbon blowdown from vessels and pipelines. Presented at SPE Annual Technical Conference and Exhibition, 25-28 September, 1993, New Orleans, Louisiana.

Peng, D., & Robinson, D. (1976). A new two-constant equation of state. *Industrial and Engineering Chemical Fundamentals*, *15*, 59-64.

Raimondi, L. (2007). Rigorous calculation of critical flow conditions for pressure safety devices. *Process Safety and Environmental Protection*, *85*(4), 277–288.

Raimondi, Luigi. (2012). Rigorous simulation of LPG releases from accidental leaks. *Chemical Engineering Transactions*, *26*, 63–68.

Richardson, S., & Saville, G. (1996). Blowdown of LPG pipelines. *Process safety and environmental protection*, *74*, 235–244.

Saha, S., & Carroll, J. J. (1997). The isoenergetic-isochoric flash. *Fluid Phase Equilibria*, *138*, 23–41.

Semantic Globe Thermal Sciences. (2010). *Critical flow*. Retrieved May 19, 2014, from Thermopedia: http://www.thermopedia.com/content/267/?tid=104&sn=1297

Whalley, P. (1987). *Boiling, condensation and gas-liquid flow.* Oxford: Clarendon Press, 163-166.

Witlox, H. W. M. & Bowen, P. (2002). Flashing liquid jets and two-phase dispersion - A review. *Contract 41003600 for HSE, Exxon-Mobil and ICI Eutech, HSE Books, Contract research report 403/2002*.

Woodward, J. L. (1990). An integrated model for discharge rate, pool spread, and dispersion from punctured process vessels. *Journal of Loss Prevention in the Process Industries*, *3*(1), 33–37.

Xia, J. L., Smith, B. L., & Yadigaroglu, G. (1993). A simplified model for depressurization of gas-filled pressure vessels. *Int. Comm. Heat Mass Transfer*, *20*(5), 653–664.